

A TIME-OPTIMAL FEEDBACK CONTROL FOR A PARTICULAR CASE OF THE GAME OF TWO CARS

ADITYA CHAUDHARI AND DEBRAJ CHAKRABORTY

ABSTRACT. In this paper, a time-optimal feedback solution to the game of two cars, for the case where the pursuer is faster and more agile than the evader, is presented. The concept of continuous subsets of the reachable set is introduced to characterize the time-optimal pursuit-evasion game under feedback strategies. Using these subsets it is shown that, if initially the pursuer is distant enough from the evader, then the feedback saddle point strategies for both the pursuer and the evader are coincident with one of the common tangents from the minimum radius turning circles of the pursuer to the minimum radius turning circles of the evader. Using geometry, four feasible tangents are identified and the feedback min – max strategy for the pursuer and the max – min strategy for the evader are derived by solving a 2×2 matrix game at each instant. Insignificant computational effort is involved in evaluating the pursuer and evader inputs using the proposed feedback control law and hence it is suitable for real-time implementation. The proposed law is validated further by comparing the resulting trajectories with those obtained by solving the differential game using numerical techniques.

1. INTRODUCTION

The problem of time optimal pursuit evasion for two Dubins vehicles or the game of two cars was first introduced by Issacs in [14]. A Dubins vehicle consists of a point moving in a plane with a given maximum forward velocity and a minimum turning radius. The problem was studied in detail in [16] for the case where evader and pursuer have equal speed and the pursuer is more agile than the evader. In recent times, numerous variants of the pursuit evasion game with Dubins vehicles have been studied. An asymmetrical version of the game of two cars is discussed in [11]. Also, variations of the homicidal chauffeur problem have been studied in [12, 20]. However, these papers aim at characterizing the regions of capture and the game of kind is solved. In most of the papers [2, 16], the optimal control law synthesis involves solving non-linear algebraic equations numerically, thereby necessitating significant computation if such laws are to be implemented as instantaneous feedback. In [21], various switching surfaces are characterized in terms of state variables, for a variation of the homicidal chauffeur game described in [20], making it possible to implement the optimal control laws as feedback. To the best of our knowledge no such time-optimal *feedback* law exists for the game of two cars, where synthesis is computationally efficient. In this paper we provide a time optimal feedback law for the special case when the pursuer is faster and more agile than the evader. We do not impose any restriction on the final orientation of the pursuer. In this case, capture by the pursuer is always guaranteed for all possible configurations of pursuer and evader [8]. Our law only involves evaluation of and comparison with closed form algebraic expressions and can be computed in real time along the trajectories, effectively providing an implementable feedback solution.

At preliminary stage of this work some results were presented in European Control Conference (ECC-2019) and some have been accepted for presentation in Conference on Decision and Control (CDC-2019).

The authors are with the Department of Electrical Engineering, Indian Institute of Technology Bombay, India. **Email:** `adityac,dc@ee.iitb.ac.in`

The optimal paths for a single Dubins vehicle have been studied extensively since [9]. Optimal control theory is used in conjunction with geometric techniques in [4, 23, 26] to characterize the curves followed by the Dubins vehicle to reach from a given initial configuration to a final configuration in minimum time, while the reachable sets of the Dubins vehicle are characterized in [6, 7]. Time optimal feedback laws have been derived for path tracking by Dubins vehicle in [22].

We use the concept of reachable set extensively in this paper. Reachable sets have been used for analyzing differential games since [8, 17]. Recently reachable sets have been used to derive feedback strategies under varying flow fields for various types of pursuers and evaders [24, 25] and also in multi-player pursuit-evasion games [13, 15, 18]. In this paper we analyze the relation between feedback min – max strategies and reachable sets. It would seem that the containment of evader’s reachable set by pursuer’s reachable set is a necessary and sufficient condition for capture under feedback strategies. However, we show that such a condition is only necessary and we establish a necessary and sufficient condition for saddle point capture in terms of some special subsets of the reachable set, which we call continuous subsets of the reachable set. Using these continuous subsets we characterize the time and point of capture under feedback strategies. From this characterization we conclude that, if the distance between the pursuer and the evader is large compared to their turning radius, then the saddle point strategies consist of a circle followed by straight line. Further, using Pontryagin’s minimum principle, we show that the trajectories are common tangents to the minimum turning radius circles of the pursuer and the evader.

Since both the vehicles are restricted to have a minimum turning radius, the pursuer and the evader each will have one clockwise minimum radius turning circle and one anti-clockwise minimum radius turning circle at each time instant. This gives us sixteen common tangents between the pursuer and evader circle pairs. Using geometrical arguments we are able to reduce the number of feasible tangents to four, one each for every pair of circles between the evader and the pursuer. A 2×2 matrix game is formulated and the min-max solution of the matrix game gives the strategy for the pursuer while the max-min solution gives the strategy for the evader. The matrix game is solved at each instant of time to obtain the feedback strategies for the differential game.

To verify and validate our control law we also solve some instances of the game of two cars numerically, using the algorithms described in [10, 19] using IPOPT [27]. In all the cases it is seen that the pursuit evasion game takes place along a common tangent to the minimum turning radius circles and the trajectory predicted by the feedback law proposed in this paper coincides with those obtained by the numerical computation of [19]. In summary, our contributions are as follows:

- (1) We introduce the concept of continuous subsets of reachable sets in order to completely characterize capture under feedback trajectories [Section 5].
- (2) If the distance between pursuer and evader is greater than a certain distance, then we show that the saddle point pursuit-evasion trajectories are coincident with a common tangent from minimum radius turning circles of pursuer to minimum radius turning circles of the evader [Section 7].
- (3) We design a computationally efficient feedback law which can be implemented in real time [Section 9].
- (4) We validate the solution obtained by our law with the one obtained by numerical simulations [Section 10].

2. PROBLEM FORMULATION

Consider a pursuer P and an evader E following the equations:

$$(2.1) \quad \begin{aligned} \dot{x}_i(t) &= v_i(t) \cos \theta_i(t) \\ \dot{y}_i(t) &= v_i(t) \sin \theta_i(t) \\ \dot{\theta}_i(t) &= v_i(t) w_i(t) \end{aligned}$$

where $i \in \{p, e\}$. The subscript p corresponds to the pursuer while e corresponds to the evader. The pursuer (evader) can control its velocity $v_i(t)$ in direction $\theta_i(t)$ and the angular velocity $w_i(t)$. We denote by $\mathcal{C}(\mathbb{R}^+, \mathbb{R}^n)$ the set of continuous functions from positive real line \mathbb{R}^+ to \mathbb{R}^n . Let $\mathbf{z}_i(t) = [x_i(t) \ y_i(t)]^\top \in \mathbb{R}^2$, $\mathbf{z}_i \in \mathcal{C}(\mathbb{R}^+, \mathbb{R}^2)$ denote the position of the pursuer (evader) in the $x - y$ plane at time t . Also, let $\theta_i(t)$ be the orientation of the pursuer (evader) in the $x - y$ plane, measured in anti-clockwise direction with respect to the $x -$ axis at time t . The complete state vector of the pursuer at time t is given by $\mathbf{p}(t) = [x_p(t) \ y_p(t) \ \theta_p(t)] \in \mathbb{R}^3$, $\mathbf{p} \in \mathcal{C}(\mathbb{R}^+, \mathbb{R}^3)$ while that of the evader is given by $\mathbf{e}(t) = [x_e(t) \ y_e(t) \ \theta_e(t)]^\top \in \mathbb{R}^3$, $\mathbf{e} \in \mathcal{C}(\mathbb{R}^+, \mathbb{R}^3)$. We also denote the projection of the pursuer's (evader's) trajectory to the $x - y$ plane corresponding to the trajectory \mathbf{p} (\mathbf{e}) by $\mathbf{z}_i = \mathbf{p}|_{\mathbb{R}^2}$ ($\mathbf{e}|_{\mathbb{R}^2}$). Let the initial state of the pursuer be denoted by $\mathbf{p}(0) = \mathbf{p}_0 = [x_{p_0} \ y_{p_0} \ \theta_{p_0}]^\top$ and that of the evader by $\mathbf{e}(0) = \mathbf{e}_0 = [x_{e_0} \ y_{e_0} \ \theta_{e_0}]^\top$. Also, let $d_{pe}(t) = \|\mathbf{z}_p(t) - \mathbf{z}_e(t)\|_2$ be the distance between pursuer and evader at time instant t and $d_{pe}(0) := d_{pe}^0$. We denote the input of the pursuer (evader) at time t by $\mathbf{u}_i(t) = [v_i(t) \ w_i(t)]^\top \in \mathbb{R}^2$ where $i \in \{p, e\}$. Also, $v_i(t) \in V_i$ where $V_i = \{v_i(t) \in \mathbb{R} : 0 \leq v_i(t) \leq v_{i_m}\}$ and $w_i(t) \in W_i$ where $W_i = \{w_i(t) \in \mathbb{R} : |w_i(t)| \leq w_{i_m}\}$ for $i \in \{p, e\}$. These restrictions limit the maximum forward velocity with which the pursuer and evader can move and also limits the rate at which the vehicles can change direction. We define the set of feasible inputs for the pursuer and the evader as $\mathbf{U}_i := \{\mathbf{u}_i(t) : v_i(t) \in V_i \text{ and } w_i(t) \in W_i\}$ where $i \in \{p, e\}$. If the input of the pursuer (evader) $\mathbf{u}_i(t) \in \mathbf{U}_i$ for all t then we write $\mathbf{u}_i \in \mathcal{U}_i$. If the pursuer (evader) sets $w_i(t) = w_{i_m}$, then it moves along a circle of radius $r_i = 1/w_{i_m}$ in anti-clockwise direction while if it applies an input of $w_i(t) = -w_{i_m}$ then it moves in clockwise direction along the circle of radius r_i .

In order to guarantee capture of evader by the pursuer, we impose the following restriction on the evader's input.

Assumption 1. *Maximum velocities of the pursuer and the evader satisfy $v_{p_m} > v_{e_m}$, while the maximum turning rates are such that $w_{p_m} > w_{e_m}$.*

In this paper, the pursuer's objective is to intercept the evader in minimum possible time, while that of the evader is to avoid interception by the pursuer for as long as possible. The complete state of the game is described by $\mathbf{x}(t) = [\mathbf{p}(t)^\top \ \mathbf{e}(t)^\top]^\top \in \mathbb{R}^6$, $\mathbf{x} \in \mathcal{C}(\mathbb{R}^+, \mathbb{R}^6)$. For capture we require that only the x and y coordinates of both the pursuer and evader must match. We do not impose the restriction that the final orientation of the pursuer and the evader must be the same. Hence, the condition at the time of capture T_c is

$$(2.2) \quad \psi(\mathbf{x}(T_c)) := \left(\begin{array}{c} x_p(t) - x_e(t) \\ y_p(t) - y_e(t) \end{array} \right) \Big|_{t=T_c} = 0$$

Thus the time of capture T_c at which the game terminates i.e. the cost function in the game of two cars, is defined by $T_c = \inf\{t \in \mathbb{R}^+ : \psi(\mathbf{x}(t)) = 0\}$. The pursuer tries to minimize T_c while the evader tries to maximize it using feedback strategies $\mathbf{u}_p := \gamma_p(\mathbf{x}) \in \mathcal{U}_p$ and $\mathbf{u}_e := \gamma_e(\mathbf{x}) \in \mathcal{U}_e$. The time to capture is a function of feedback strategy pair $(\gamma_p(\mathbf{x}), \gamma_e(\mathbf{x}))$ and we denote it by $T_c(\gamma_p(\mathbf{x}), \gamma_e(\mathbf{x}))$. The pursuer must guard against the worst-case strategies of the evader. Hence, the minimum time capture problem for the pursuer is a min - max time-optimal problem. So the pursuer's problem is:

Problem 2. Find $\mathbf{u}_p = \gamma_p^*(\mathbf{x})$ which solves

$$\gamma_{\mathbf{p}}^*(\mathbf{x}) = \operatorname{argmin}_{\gamma_{\mathbf{p}}} \max_{\gamma_{\mathbf{e}}} T_c(\gamma_{\mathbf{p}}(\mathbf{x}), \gamma_{\mathbf{e}}(\mathbf{x}))$$

Similarly, the evader must guard against every possible strategy of the pursuer. Thus, the maximum time evasion problem for the evader is to find the max – min strategy of the evader.

Problem 3. Find $\mathbf{u}_{\mathbf{e}}(t) = \gamma_{\mathbf{e}}^*(\mathbf{x})$ which solves

$$\gamma_{\mathbf{e}}^*(\mathbf{x}) = \operatorname{argmax}_{\gamma_{\mathbf{e}}} \min_{\gamma_{\mathbf{p}}} T_c(\gamma_{\mathbf{p}}(\mathbf{x}), \gamma_{\mathbf{e}}(\mathbf{x}))$$

Such problems have been studied extensively in the theory of differential games where the solutions of both Problem 2 and Problem 3 are characterized in terms of saddle-point strategies and the value of the game [1, 5, 14].

Definition 4. A *feedback strategy pair* $(\gamma_{\mathbf{p}}^*, \gamma_{\mathbf{e}}^*)$ is said to be a saddle-point equilibrium if

$$(2.3) \quad T_c(\gamma_{\mathbf{p}}^*, \gamma_{\mathbf{e}}) \leq T_c(\gamma_{\mathbf{p}}^*, \gamma_{\mathbf{e}}^*) \leq T_c(\gamma_{\mathbf{p}}, \gamma_{\mathbf{e}}^*)$$

$\forall \gamma_{\mathbf{e}}(\mathbf{x}) \in \mathbf{U}_{\mathbf{e}}, \gamma_{\mathbf{p}}(\mathbf{x}) \in \mathbf{U}_{\mathbf{p}}$ and the value of the game, if it exists, is $T^* := T_c(\gamma_{\mathbf{p}}^*, \gamma_{\mathbf{e}}^*)$.

In the game of two cars considered above, under Assumption 1, the following result holds.

Theorem 5. [8] *If Assumption 1 holds, there exists a pursuer input $\mathbf{u}_{\mathbf{p}} := \gamma_{\mathbf{p}}(\mathbf{x})$ such that for all $\mathbf{u}_{\mathbf{e}} := \gamma_{\mathbf{e}}(\mathbf{x})$, capture is guaranteed i.e. $\psi(\mathbf{x}(T_c)) = 0$ for some $T_c(\gamma_{\mathbf{p}}(\mathbf{x}), \gamma_{\mathbf{e}}(\mathbf{x})) < \infty$.*

Since the capture is guaranteed and the Hamiltonian (considered later in Section 8.2) is separable in pursuer’s input and evader’s input, the existence of saddle point strategies $(\gamma_{\mathbf{p}}^*, \gamma_{\mathbf{e}}^*)$ follows [5]. This implies that $\mathbf{u}_{\mathbf{p}}^* := \gamma_{\mathbf{p}}^*(\mathbf{x})$ and $\mathbf{u}_{\mathbf{e}}^* := \gamma_{\mathbf{e}}^*(\mathbf{x})$ are the solutions of Problem 2 and 3 respectively with $T^* = T_c(\gamma_{\mathbf{p}}^*, \gamma_{\mathbf{e}}^*) < \infty$.

3. PRELIMINARIES

3.1. Minimum radius turning circles and common tangents. In this section we define the minimum radius turning circles of the pursuer and evader and also the common tangents. These tangents will be used to derive feedback laws for the time-optimal pursuit-evasion game of two cars.

Definition 6. *Clockwise pursuer-circle (evader-circle), $C_i(\bar{t})$, at time \bar{t} is the clockwise circle of radius $r_i = \frac{1}{w_{i_m}}$ and center $(x_c(\bar{t}) = x(\bar{t}) + \sin(\theta(\bar{t}))/w_{i_m}, y_c(\bar{t}) = y(\bar{t}) - \cos(\theta(\bar{t}))/w_{i_m})$ that the pursuer (evader) follows when $w_i(t) = -w_{i_m} \forall t \geq \bar{t}$, where $i \in \{p, e\}$.*

Definition 7. *Anti-clockwise pursuer-circle (evader-circle), $A_i(\bar{t})$, at time \bar{t} is the anti-clockwise circle of radius $r_i = \frac{1}{w_{i_m}}$ and center $(x_c(\bar{t}) = x(\bar{t}) - \sin(\theta(\bar{t}))/w_{i_m}, y_c(\bar{t}) = y(\bar{t}) + \cos(\theta(\bar{t}))/w_{i_m})$ that the pursuer (evader) follows when $w_i(t) = +w_{i_m} \forall t \geq \bar{t}$, where $i \in \{p, e\}$.*

Remark 8. These circles for a particular position of the pursuer (evader) are shown in Figure 3.1 and will be called the pursuer-circles (evader-circles). These circles are also called the minimum radius turning circles of Dubins vehicle. Note that, the expression of $\dot{\theta}$ in (2.1) has the velocity term multiplied. This results in turning radius being independent of $v_i(t)$ and depends only on $w_i(t)$. Thus for $w_i(t) = w$ for $t \in [t_1, t_2]$ the vehicle will move along an arc of a circle of radius $r_i = 1/w$ with velocity $v_i(t)$ for the duration $[t_1, t_2]$. If the input $w_i(t) = 0$ and $v_i(t) \in (0, v_{i_m}]$ for $i \in \{p, e\}$ in the time interval $[t_1, t_2]$ then the pursuer (evader) moves in a straight line during this time interval.

In order to design feedback laws we make use of the common tangents from the pursuer-circles to the evader-circles. Note that the pursuer-circles (evader-circles) at time t depend only on the position and orientation of the pursuer (evader) at time instant t . Let $OC(t)$ denote the set of pursuer-circles and evader-circles at time t .

$$OC(t) := \{A_p(t), C_p(t), A_e(t), C_e(t)\}$$

A PE -pair is a pair of circles with one circle belonging to the pursuer-circles and the other circle belonging to the evader-circles. Thus, in total we have four PE -pairs. The set of PE -pairs at time t is denoted by $PE(t)$.

$$PE(t) = \{\{C_p(t), C_e(t)\}, \{C_p(t), A_e(t)\}, \\ \{A_p(t), C_e(t)\}, \{A_p(t), A_e(t)\}\}$$

Between the two circles belonging to a PE -pair, whose centers are at a minimum distance of $r_p + r_e$ away from each other, there will be four tangents. These tangents have been shown in between the PE -pair $\{A_p(t), C_e(t)\}$ in Figure 3.1. We assign direction to the tangents from the pursuer to the evader and we call them directed common tangents.

Definition 9. Valid common tangent for a PE – pair is a directed common tangent whose orientation matches with the direction of both the pursuer circle and the evader circle in the PE – pair.

In Figure 3.1 only the tangent T_3 (shown by dashed line) is a valid tangent for pair $\{A_p(t), C_e(t)\}$.

Definition 10. If a pursuer’s (evader’s) trajectory up to some time $t_f > 0$ is such that it traverses one of the pursuer-circles (evader-circles) in time interval $[0, t']$ with $t' \leq \min(t_f, 2\pi r_p/v_{p_m})$, and then traverses one of the tangents to that pursuer-circle (evader-circle) in time interval $[t', t_f]$, then such a trajectory is of the type CS (circle and straight line) up to time t_f .

Remark 11. The condition $t' \leq 2\pi r_p/v_{p_m}$ ensures that no part along the circumference of the circle is traversed more than once. If a trajectory of type CS follows anticlockwise (left) circle and after that follows a straight line path then we say the trajectory belongs to the type LS . Similarly, if it follows clockwise (right) circle and after that follows a straight line path then we say the trajectory is of the type RS .

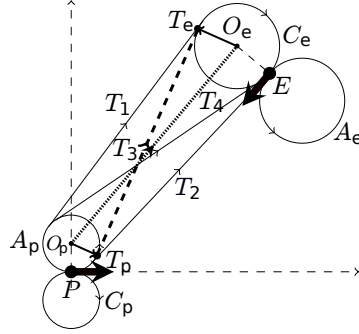
Definition 12. If a pursuer’s (evader’s) trajectory up to time t_f is such that it traverses one of the pursuer-circles (evader-circles) say $A_p(0)$ ($A_e(0)$) in time interval $[0, t']$ with $t' \leq \min(t_f, 2\pi r_p/v_{p_m})$, and then traverses the other pursuer-circle (evader-circle) i.e. $C_p(0)$ ($C_e(0)$) in the time interval $[t', t_f]$, then such a trajectory is of the type CC (circle-circle).

3.2. Reachable Sets. We use reachable sets in order to characterize the nature of saddle point trajectories.

Definition 13. [7] The reachable set of pursuer (evader), denoted by $R_p(\mathbf{p}_0, \bar{t}) \subset \mathbb{R}^2$ ($R_e(\mathbf{e}_0, \bar{t}) \subset \mathbb{R}^2$), at time \bar{t} from initial state $\mathbf{p}(0) = \mathbf{p}_0$ ($\mathbf{e}(0) = \mathbf{e}_0$), is the set of all points that can be reached in time $t \leq \bar{t}$ by applying inputs $\mathbf{u}_p \in \mathcal{U}_p$ ($\mathbf{u}_e \in \mathcal{U}_e$).

$$R_p(\mathbf{p}_0, \bar{t}) = \{\mathbf{z} \in \mathbb{R}^2 : \exists \mathbf{u}_p \in \mathcal{U}_p \text{ and corresponding} \\ \text{trajectory } \mathbf{p} \in \mathcal{C}(\mathbb{R}^+, \mathbb{R}^3) \text{ s.t.} \\ \mathbf{p}|_{\mathbb{R}^2}(t) = \mathbf{z} \text{ for some } t \leq \bar{t} \text{ and } \mathbf{p}(0) = \mathbf{p}_0\}$$

The reachable set for the Dubins vehicle has been studied in [6, 7]. It is known that, the points inside the pursuer (evader) circles can be reached in minimum time by CC (circle-circle) types of curves. The points external to the pursuer (evader) circles can be reached in minimum time by CS type of curves. The external boundary of $R_p(\mathbf{p}_0, \bar{t})$ ($R_e(\mathbf{e}_0, \bar{t})$) is denoted by $\partial R_p(\mathbf{p}_0, \bar{t})$ ($\partial R_e(\mathbf{e}_0, \bar{t})$).


 FIGURE 3.1. Common Tangents $\{A_p(t), C_e(t)\}$

It is known [6] that, if $\bar{t} \geq 2\pi r_p/v_{p_m}$ ($\bar{t} \geq 2\pi r_e/v_{e_m}$) the points on $\partial R_p(\mathbf{p}_0, \bar{t})$ ($\partial R_e(\mathbf{e}_0, \bar{t})$) at time \bar{t} can be reached only by the trajectories of the type *CS*. Thus $\partial R_p(\mathbf{p}_0, \bar{t})$ ($\partial R_e(\mathbf{e}_0, \bar{t})$) at $\bar{t} \geq 2\pi r_p/v_{p_m}$ ($\bar{t} \geq 2\pi r_e/v_{e_m}$) is comprised of two portions. The first portion is characterized by trajectories which begin on anti-clockwise circle and then follow a straight line. The second portion is characterized by trajectories which begin on the clockwise circle and then follow a straight line.

Consider the pursuer with initial state vector $\mathbf{p}(0) = [x_0 \ y_0 \ \theta_0]^\top$. The trajectories $\mathbf{p} \in \mathcal{C}(\mathbb{R}^+, \mathbb{R}^3)$ corresponding to the input

$$\begin{aligned} w_p(t) &= +w_{p_m} \quad t \in [0, t_1] \\ &= 0 \quad t \in (t_1, \bar{t}] \\ v_p(t) &= v_{p_m} \quad t \in [0, \bar{t}] \end{aligned}$$

for some $0 \leq t_1 \leq 2\pi r_p/v_{p_m}$, will initially follow the anti-clockwise circle and then travel on a tangent to the anti-clockwise circle. (Note that the switching time t_1 is less than $2\pi r_p/v_{p_m}$ so that the no length of the circle is repeated). The trajectory is parameterized by the switching time t_1 and can be obtained by integrating (2.1) as

$$\begin{aligned} x_{fl}(\bar{t}) &= x_0 + (\sin(\theta_0 + v_{p_m} w_{p_m} t_1) - \sin(\theta_0))/w_{p_m} \\ &\quad + v_{p_m} \cos(\theta_0 + v_{p_m} w_{p_m} t_1)(\bar{t} - t_1) \\ y_{fl}(\bar{t}) &= y_0 - (\cos(\theta_0 + v_{p_m} w_{p_m} t_1) - \cos(\theta_0))/w_{p_m} \\ &\quad + v_{p_m} \sin(\theta_0 + v_{p_m} w_{p_m} t_1)(\bar{t} - t_1) \end{aligned} \quad (3.1)$$

Using these expressions the left reachable set of pursuer is defined as

$$\begin{aligned} R_p^l(\mathbf{p}_0, \bar{t}) &= \{\mathbf{z} = [x \ y]^\top \in \mathbb{R}^2 \mid x = x_{fl}(\bar{t}) \\ &\quad \text{and } y = y_{fl}(\bar{t}) \ \forall t_1 \leq \bar{t}\} \end{aligned}$$

The left reachable set for the evader $R_e^l(\mathbf{e}_0, \bar{t})$ is defined analogously. The left reachable set is shown in Figure 3.2. The boundary of left reachable set of pursuer (evader) is denoted by $\partial R_p^l(\mathbf{p}_0, \bar{t})$ ($\partial R_e^l(\mathbf{e}_0, \bar{t})$).

For $\bar{t} \geq 2\pi r_p/v_{p_m}$ the right reachable sets for the pursuer $R_p^r(\mathbf{p}_0, \bar{t})$ and evader $R_e^r(\mathbf{e}_0, \bar{t})$ are defined similarly by the trajectories which first travel on the clockwise circle and then on the tangent to the clockwise circle. The right reachable set is shown in Figure 3.3. The boundary of right reachable set of pursuer (evader) is denoted by $\partial R_p^r(\mathbf{p}_0, \bar{t})$ ($\partial R_e^r(\mathbf{e}_0, \bar{t})$).

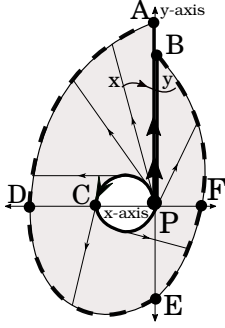


FIGURE
3.2. Left
reachable set

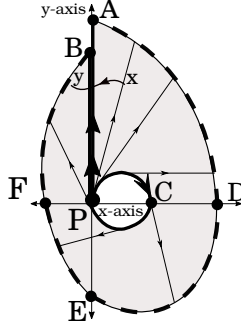


FIGURE
3.3. Right
reachable set

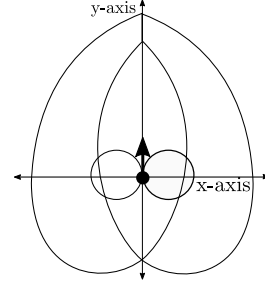


FIGURE
3.4. $R_p^r(\mathbf{p}_0, \bar{t}) \cup$
 $R_p^l(\mathbf{p}_0, \bar{t})$

The left reachable set and right reachable set of the pursuer (evader) are the subsets of the reachable set $R_p(\mathbf{p}_0, \bar{t})$ ($R_e(\mathbf{e}_0, \bar{t})$). The union of $R_p^l(\mathbf{p}_0, \bar{t})$ and $R_p^r(\mathbf{p}_0, \bar{t})$ is shown in Figure 3.4.

The boundary of left reachable set is divided in two parts for $\bar{t} \geq 2\pi r_p/v_{p_m}$ in next definition.

Definition 14. For $\bar{t} \geq 2\pi r_p/v_{p_m}$, the portion ADE as shown in Figure 3.2 will be called the *left external boundary* whereas the portion EFB will be called the *left internal boundary*. Similarly, for the right reachable set the portion ADE as shown in Figure 3.3 will be called the *right external boundary* whereas the portion EFB will be called the *right internal boundary* for $\bar{t} \geq 2\pi r_p/v_{p_m}$.

Remark 15. The external boundary of the reachable set $\partial R_p(\mathbf{p}_0, \bar{t})$ ($\partial R_e(\mathbf{e}_0, \bar{t})$) is the union of left external boundary and the right external boundary for $\bar{t} \geq 2\pi r_p/v_{p_m}$. Note that the shape of the reachable sets is as shown in Figures 3.2, 3.3, 3.4 only if $\bar{t} \geq 2\pi r_e/v_{e_m} \geq 2\pi r_p/v_{p_m}$.

4. ANALYSIS USING REACHABILITY SETS

The reachability set characterizes the points which the Dubins vehicle can reach in a given time. It would seem that the evader can always escape capture if the evader's reachable set is not contained completely inside the pursuer's reachable set. However, this is only possible if there exists an evader trajectory which can enter the region not contained in pursuer's reachable set, without passing through the pursuer's reachable set. For if the trajectory passes through the pursuer's reachable set it will be intercepted by some pursuer's trajectory. This notion is formalized in the next definition by introducing the safe region of the evader with respect to subsets of pursuer's reachable set.

Definition 16. The *safe region* of the evader, at time \bar{t} , with respect to a subset of pursuer's reachable set $R_p^s(\mathbf{p}_0, \bar{t}) \subset R_p(\mathbf{p}_0, \bar{t})$ is defined as

$$R_e^-(\mathbf{e}_0, R_p^s, \bar{t}) = \{ \mathbf{z} \in \mathbb{R}^2 : \mathbf{z} \in R_e(\mathbf{e}_0, \bar{t}) \setminus R_p^s(\mathbf{p}_0, \bar{t}) \\ \text{and } \exists \text{ an evader trajectory} \\ \text{with } \mathbf{e}_{|\mathbb{R}^2}(t_1) = \mathbf{z} \text{ for some } t_1 \leq \bar{t}, \\ \text{and } \mathbf{e}_{|\mathbb{R}^2}(t) \notin R_p^s(\mathbf{p}_0, t) \forall t \leq \bar{t} \}$$

Lemma 17. Let T_l be the minimum time such that $R_e^-(\mathbf{e}_0, R_p^l, T_l) = \emptyset$. If $d_{pe}^0 \geq 2r_p + 2\pi r_p(v_{e_m}/v_{p_m})$ then $T_l < \infty$.

Proof. See Appendix. □

Similarly, we have the following lemma for $R_p^r(\mathbf{p}_0, \bar{t})$.

Lemma 18. *Let T_r be the minimum time such that $R_e^-(\mathbf{e}_0, R_p^r, T_r) = \emptyset$. If $d_{pe}^0 \geq 2r_p + 2\pi r_p(v_{e_m}/v_{p_m})$ then $T_r < \infty$.*

Lemma 19. *Let T_o be the minimum time such that $R_e^-(\mathbf{e}_0, R_p, T_o) = \emptyset$. If $d_{pe}^0 \geq 2r_p + 2\pi r_p(v_{e_m}/v_{p_m})$ then $T_o < \infty$.*

Proof. Follows from Lemma 17 and Lemma 18. □

Remark 20. It would seem that the condition $R_e^-(\mathbf{e}_0, R_p, \bar{t}) = \emptyset$, would be necessary and sufficient for capture. Let $T_o = \inf\{t \in \mathbb{R} : R_e^-(\mathbf{e}_0, R_p, t) = \emptyset\}$. It is shown in [24], for pursuer and evader which can turn instantaneously, that such a condition is indeed necessary and sufficient for capture if we consider open-loop strategies and capture occurs at T_o . However, the claim does not hold if we consider feedback strategies for the pursuer and evader. We demonstrate that $R_e^-(\mathbf{e}_0, R_p, T_o) = \emptyset$ is not a sufficient condition for capture under feedback strategies in the following counter examples.

Example 21. Refer to Figure 4.1 where the evader is exactly behind the pursuer and oriented away from the pursuer. At some time T_o , the evader's reachable set (dotted curve) is contained in pursuer's reachable set (solid line). If $R_e^-(\mathbf{e}_0, R_p, T_o) = \emptyset$ was the criterion for capture, then the evader would have traveled straight and the pursuer would have intercepted it along the CS path exactly at the point marked by star in Figure 4.1. However, the optimal feedback strategies obtained by numerical simulation (using the algorithms in [10, 19]) and the reachable set for such a strategy are as shown in Figure 4.2. It can be seen that the trajectory is a common tangent between the pursuer and evader circles and the capture occurs when the left reachable set contains the evader's reachable set. Hence, $R_e^-(\mathbf{e}_0, R_p, T_o) = \emptyset$ is not a sufficient criterion for capture.

Example 22. An alternate hypothesis, might be that capture occurs when either the left reachable set or the right reachable set completely contains the evader's reachable region as shown in Figure 4.2. But consider the case when evader is in front of the pursuer as shown in Figure 4.3. Again the game is solved numerically using algorithms in [10, 19]. At the point of capture, marked by the star, neither the left nor the right reachable set of the pursuer contain the evader's reachable set.

In order to resolve the issue of capture in terms of reachable sets, we introduce the notion of continuous subsets of reachable sets.

5. CONTINUOUS SUBSETS OF REACHABLE SET

Recall that $T_o = \inf\{t \in \mathbb{R} : R_e^-(\mathbf{e}_0, R_p, t) = \emptyset\}$ and consider a point $\mathbf{z} \in \partial R_e(\mathbf{e}_0, T_o) \cap \partial R_p(\mathbf{p}_0, T_o)$. In Example 21 it was shown that the capture did not occur at point \mathbf{z} . We try to explain this phenomena using small deviations around the evader input signal. This will result in a small deviation in the final point $\mathbf{e}_{\mathbb{R}^2}(T_o) = \mathbf{z}$. Now if capture is to occur at $\mathbf{z} = \mathbf{e}_{\mathbb{R}^2}(T_o)$, using feedback pursuer strategies, every feasible variation in \mathbf{e} should be *traceable* by the pursuer using small variations of its own input signal. We make the notion of admissible variations more concrete in this section by defining the continuous subsets of the reachable set for the Dubins vehicle.

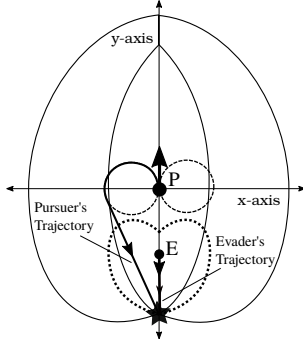


FIGURE 4.1. Invalid containment of evader's reachable set

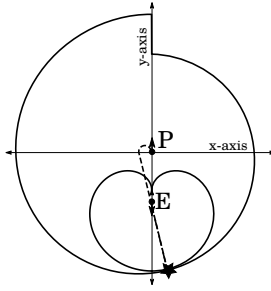


FIGURE 4.2. Valid containment of evader's reachable set

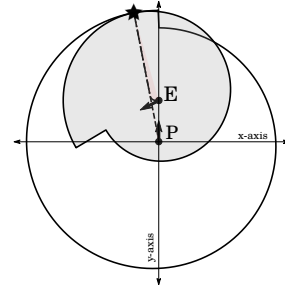


FIGURE 4.3. Left reachable set does not contain evader's reachable set. Yet capture occurs at this time.

Definition of Continuous Subsets of Reachable Sets. Let $R_p(\mathbf{p}_0, \bar{t})$ be the reachable set of the pursuer at time \bar{t} starting from initial position $\mathbf{p}_0 \in \mathbb{R}^3$.

- (1) Let $\mathbf{x}, \mathbf{y} \in R_p(\mathbf{p}_0, \bar{t})$ and let $\overline{\mathbf{x}\mathbf{y}}$ be any curve from \mathbf{x} to \mathbf{y} such that all points on $\overline{\mathbf{x}\mathbf{y}}$ belong to $R_p(\mathbf{p}_0, \bar{t})$ as shown in Figure 5.1.
- (2) Let $\mathfrak{T}_{\overline{\mathbf{x}\mathbf{y}}}(\mathbf{r}, \mathbf{p}_0, \bar{t})$ be the set of all the trajectories from \mathbf{p}_0 to the point \mathbf{r} on $\overline{\mathbf{x}\mathbf{y}}$, which reach the point $\mathbf{r} \in R_p(\mathbf{p}_0, \bar{t})$ at time $t \leq \bar{t}$ starting from \mathbf{p}_0 .

$$\mathfrak{T}_{\overline{\mathbf{x}\mathbf{y}}}(\mathbf{r}, \mathbf{p}_0, \bar{t}) = \{ \mathbf{p} \in C^0(\mathbb{R}^+, \mathbb{R}^3) : \exists \mathbf{u}_p \in \mathcal{U}_p \text{ with} \\ \mathbf{p}|_{\mathbb{R}^2}(t) = \mathbf{r} \text{ and } \mathbf{p}(0) = \mathbf{p}_0 \text{ for} \\ \text{some } t \leq \bar{t} \}$$

- (3) Let $\mathfrak{L}(\overline{\mathbf{x}\mathbf{y}}, \mathbf{p}_0, \bar{t})$ be the collection of all possible trajectories from \mathbf{p}_0 which reach line $\overline{\mathbf{x}\mathbf{y}}$ at time $t \leq \bar{t}$.

$$\mathfrak{L}(\overline{\mathbf{x}\mathbf{y}}, \mathbf{p}_0, \bar{t}) = \left\{ \mathbf{p} \in C^0(\mathbb{R}^+, \mathbb{R}^3) : \exists \mathbf{r} \in \overline{\mathbf{x}\mathbf{y}} \right. \\ \left. \text{s.t. } \mathbf{p} \in \mathfrak{T}_{\overline{\mathbf{x}\mathbf{y}}}(\mathbf{r}, \mathbf{p}_0) \right\}$$

- (4) Now we look at functions $f : \overline{\mathbf{x}\mathbf{y}} \rightarrow \mathfrak{L}(\overline{\mathbf{x}\mathbf{y}}, \mathbf{p}_0, \bar{t})$ such that $f(\mathbf{r}) \in \mathfrak{T}_{\overline{\mathbf{x}\mathbf{y}}}(\mathbf{r}, \mathbf{p}_0, \bar{t}) \forall \mathbf{r} \in \overline{\mathbf{x}\mathbf{y}}$. We construct a set $\mathfrak{C}(\overline{\mathbf{x}\mathbf{y}}, \mathbf{p}_0, \bar{t})$ such that

$$\mathfrak{C}(\overline{\mathbf{x}\mathbf{y}}, \mathbf{p}_0, \bar{t}) = \{ f | f : \overline{\mathbf{x}\mathbf{y}} \rightarrow \mathfrak{L}(\overline{\mathbf{x}\mathbf{y}}, \mathbf{p}_0, \bar{t}) \\ \text{and } f(\mathbf{r}) \in \mathfrak{T}_{\overline{\mathbf{x}\mathbf{y}}}(\mathbf{r}, \mathbf{p}_0, \bar{t}) \\ \forall \mathbf{r} \in \overline{\mathbf{x}\mathbf{y}} \}$$

The set $\mathfrak{C}(\overline{\mathbf{x}\mathbf{y}}, \mathbf{p}_0, \bar{t})$ is the set of all the functions which map some point $\mathbf{r} \in \overline{\mathbf{x}\mathbf{y}}$ to a trajectory $\mathbf{p} \in \mathfrak{L}(\overline{\mathbf{x}\mathbf{y}}, \mathbf{p}_0, \bar{t})$ and the trajectory \mathbf{p} is such that $\mathbf{p}|_{\mathbb{R}^2}(\bar{t}) = \mathbf{r}$.

- (5) Let the metric be defined on set $\overline{\mathbf{x}\mathbf{y}}$ by the standard two norm. The metric on the set $\mathfrak{L}(\overline{\mathbf{x}\mathbf{y}}, \mathbf{p}_0, \bar{t})$ is defined by the \mathcal{L}_∞ norm.

Definition 23. We say that the curve $\overline{\mathbf{x}\mathbf{y}}$ is a *continuum set* if there exists a continuous one-one map $\mathbf{f}^c \in \mathfrak{C}(\overline{\mathbf{x}\mathbf{y}}, \mathbf{p}_0, \bar{t})$.

Definition 24. The range of \mathbf{f}^c will be called the *continuum of trajectories*.

Remark 25. Since, \mathbf{f}^c is a continuous function, the trajectories in the continuum of trajectories of \mathbf{f}^c are such that for any two points $\mathbf{w}, \mathbf{z} \in \overline{\mathbf{x}\mathbf{y}}$ we have $\|\mathbf{f}^c(\mathbf{w}) - \mathbf{f}^c(\mathbf{z})\|_{\mathcal{L}_\infty} \rightarrow 0$ as $\|\mathbf{w} - \mathbf{z}\|_2 \rightarrow 0$.

Definition 26. A *continuous subset* of the reachable set at time \bar{t} , $R_p^c(\mathbf{p}_0, \bar{t}) \subseteq R_p(\mathbf{p}_0, \bar{t})$ is a connected set of all the points s.t.

- (1) For all $\mathbf{x}, \mathbf{y} \in R_p^c(\mathbf{p}_0, \bar{t})$ and every curve $\overline{\mathbf{x}\mathbf{y}} \in R_p^c(\mathbf{p}_0, \bar{t})$, the set $\overline{\mathbf{x}\mathbf{y}}$ is a continuum set.
- (2) For every point $\mathbf{r} \in R_p^c(\mathbf{p}_0, \bar{t})$ there exists a trajectory $\mathbf{p} \in \mathcal{C}^0(\mathbb{R}^+, \mathbb{R}^3)$ such that $\mathbf{p}(0) = \mathbf{p}_0, \mathbf{p}(\bar{t}) = \mathbf{r}$ for some $0 \leq \tilde{t} \leq \bar{t}$ and $\mathbf{p}(t) \in R_p^c(\mathbf{p}_0, \bar{t})$ for all $t \leq \tilde{t}$.

Definition 27. Let $\overline{\mathbf{x}\mathbf{y}}$ be a continuum set. If a continuum of trajectories for the curve $\overline{\mathbf{x}\mathbf{y}}$ are of the type *LS* then we say that $\overline{\mathbf{x}\mathbf{y}}$ is a *LS continuum set*. *RS, CS* continuum sets are defined analogously.

From here on we will denote a continuous subset of pursuer's reachable set by *CSP*. A continuous subset of the reachable set of the evader is defined analogously and will be denoted by *CSE*.

Lemma 28. Let $\bar{t} \geq 2\pi r_p/v_{p_m}$ and consider Figure 3.2. Any curve $\overline{\mathbf{x}\mathbf{y}} \in R_p^l(\mathbf{p}_0, \bar{t})$ such that $\overline{\mathbf{x}\mathbf{y}}$ crosses the line *PA*, is not a *LS* continuum set.

Proof. Recall that the switching time t_1 for *LS* type trajectory is less than $2\pi r_p/v_{p_m}$. The portion of the curve $\overline{\mathbf{x}\mathbf{y}}$ on the left of *PA* can be reached by *LS* trajectories which have switching time $t_1 \leq \pi r_p/v_{p_m}$ while the portion on right of *PA* can be reached by curves with switching time $t_1 \geq (3\pi/2)r_p/v_{p_m}$. Hence, there do not exist *LS* trajectories which can make $\overline{\mathbf{x}\mathbf{y}}$ a continuum set. \square

Lemma 29. Let $\bar{t} \geq 2\pi r_p/v_{p_m}$. Consider Figure 5.1. Any curve $\overline{\mathbf{x}\mathbf{y}} \in R_p^l(\mathbf{p}_0, \bar{t}) \setminus PA$ is a *LS* continuum set.

Proof. Recall that the switching time t_1 for a *LS* trajectory is less than $2\pi r_p/v_{p_m}$. Consider any curve $\overline{\mathbf{x}\mathbf{y}}$ between points $\mathbf{x}, \mathbf{y} \in R_p^l(\mathbf{p}_0, \bar{t}) \setminus PA$ as shown in Figure 5.1. Let \mathbf{p}_x be the trajectory of the type *LS* given by (3.1) and $\mathbf{x} = \mathbf{p}_x|_{\mathbb{R}^2}(t_a) = [x_{fl}(t_a) \ y_{fl}(t_a)]^\top$ for some $t_a \leq \bar{t}$. Let \mathbf{x}' be a point in neighborhood of \mathbf{x} such that $\mathbf{x}' = \mathbf{x} + \delta\mathbf{x}$ and $\mathbf{x}' \in \overline{\mathbf{x}\mathbf{y}}$. Since, (3.1) are differentiable in t_a , they are continuous in t_a and the point \mathbf{x}' can be reached at $t_a + \delta t_a$ by a *LS* trajectory, say $\mathbf{p}_{x'}$. Further, since the function is continuous in t_1 , for $t_1 < 2\pi r_p/v_{p_m}$ (by Lemma 28), the switching time is $t_1 + \delta t_1$ for some *LS* trajectory. By continuity we have $\delta t_a \rightarrow 0, \delta t_1 \rightarrow 0$ as $\delta\mathbf{x} \rightarrow 0$. Since, the switching time changes only by small amount, $\|\mathbf{p}_x - \mathbf{p}_{x'}\|_{\mathcal{L}_\infty} \rightarrow 0$. Define a function \mathbf{f} such that it matches each point \mathbf{x} to the trajectory of the type *CS* given by (3.1) and $\mathbf{x} = \mathbf{p}_x|_{\mathbb{R}^2}(t_a) = [x_{fl}(t_a) \ y_{fl}(t_a)]$ for some $t_a \leq \bar{t}$. Thus the function \mathbf{f} would be a one-one function by definition. Further, the function is also continuous by the analysis presented above. Thus $\overline{\mathbf{x}\mathbf{y}}$ is a continuum set. \square

The following lemma is analogous to Lemma 29.

Lemma 30. Let $\bar{t} \geq 2\pi r_p/v_{p_m}$. Any curve $\overline{\mathbf{x}\mathbf{y}} \in R_p^r(\mathbf{p}_0, \bar{t}) \setminus PA$ is a *RS* continuum set.

Next, we define a series of special continuous subsets of reachable sets, which will be useful to characterize the saddle point capture condition in Section 7.1 and Section 7.2.

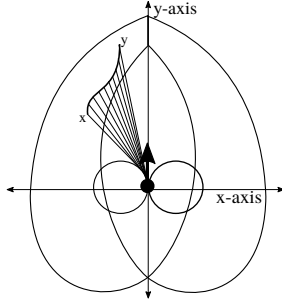


FIGURE 5.1. Continuum of trajectories

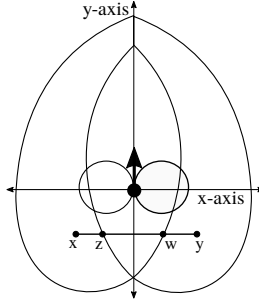


FIGURE 5.2. $R_p^r(\mathbf{p}_0, \bar{t}) \cup R_p^l(\mathbf{p}_0, \bar{t})$ is not a CSP.

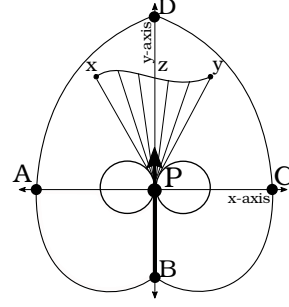


FIGURE 5.3. Central reachable set is a continuous subset

Definition 31. Let $\bar{t} \geq 2\pi r_p/v_{p_m}$. Then, the **central reachable set** of the pursuer (see Figure 5.3) is defined as $R_p^{CR}(\mathbf{p}_0, \bar{t}) = R_p(\mathbf{p}_0, \bar{t})/\{\text{int}(C_p(0)) \cup \text{int}(A_p(0)) \cup \overline{PB}\}$, where $\text{int}(C_p(0))$ and $\text{int}(A_p(0))$ denote the interiors of pursuer circles at time $t = 0$ and $\overline{PB} = \{PB/\{P\}\}$.

The central reachable set of the evader $R_e^{CR}(\mathbf{e}_0, \bar{t})$ is defined analogously for $\bar{t} \geq 2\pi r_e/v_{e_m}$. The central reachable set is shown in Figure 5.3. The points on the line segment \overline{PB} and the area inside the minimum turning radius circles do not form a part of central reachable set.

Lemma 32. *The central reachable set of pursuer/evader is a continuous subset for all time $t \geq 2\pi \frac{r_p}{v_{p_m}}$ ($t \geq 2\pi \frac{r_e}{v_{e_m}}$).*

Proof. Consider Figure 5.3. Let D_l denote the set of points enclosed by the curve $DABPD$ and D_r be the set of points enclosed by the curve $DCBPD$. Any curve contained completely in the set $D_l \setminus (\overline{PB} \cup \text{int}(A_p(0))) \subseteq R_p^l(\mathbf{p}_0, \bar{t})$ is a continuum set by Lemma 29. Similarly, any curve that is contained completely in the set $D_r \setminus (\overline{PB} \cup \text{int}(A_p(0))) \subseteq R_p^r(\mathbf{p}_0, \bar{t})$ is a continuum set by Lemma 30. Thus we need to consider only those type of curves which cross line DP such as the curve $\mathbf{x} - \mathbf{z} - \mathbf{y}$ shown in Figure 5.3. The curve $\mathbf{x}\mathbf{z}$ in Figure 5.3 is a *LS* continuum set. Let this continuum set of trajectories be denoted by \mathbf{T}^l . Similarly, any curve $\mathbf{z}\mathbf{y}$ in the subset $DCBPD \subseteq R_p^r(\mathbf{p}_0, \bar{t})$ as shown in Figure 5.3 is a continuous subset with *RS* type of trajectories. Let this continuum of trajectories be denoted by \mathbf{T}^r . Now, the trajectory in \mathbf{T}^l and \mathbf{T}^r which reaches the point \mathbf{z} is the same trajectory along the straight line PD . Thus, $\mathbf{T}^l \cup \mathbf{T}^r$ forms a continuum of trajectories for the curve $\mathbf{x} - \mathbf{z} - \mathbf{y}$ and hence it is a continuum set. Thus any curve in the central reachable set is a continuum set with *CS* type of trajectories. Further, the continuum of trajectories $\mathbf{T}^l \cup \mathbf{T}^r$ is completely contained in $R_p^{CR}(\mathbf{p}_0, \bar{t})$. Hence, the central reachable set it is a continuous subset. \square

Definition 33. Consider Figures 3.2 and 3.3 and let $\bar{t} \geq 2\pi r_p/v_{p_m}$. The **truncated left reachable set** is defined as $R_p^{lt}(\mathbf{p}_0, \bar{t}) := R_p^l(\mathbf{p}_0, \bar{t})/PA$. Similarly, the **truncated right reachable set** is defined as $R_p^{rt}(\mathbf{p}_0, \bar{t}) = R_p^r(\mathbf{p}_0, \bar{t})/PA$.

The truncated left reachable set and the truncated right reachable set for the evader are defined analogously. The proofs of Lemma 34 and Lemma 35 follow from Lemma 29 and Lemma 30.

Lemma 34. *Pursuer's (Evader's) truncated left reachable set $R_p^{lt}(\mathbf{p}_0, \bar{t})$ ($R_e^{lt}(\mathbf{e}_0, \bar{t})$) is a continuous subset for all $t \geq 2\pi \frac{r_p}{v_{p_m}}$ ($t \geq 2\pi \frac{r_e}{v_{e_m}}$).*

Lemma 35. Pursuer's (Evader's) truncated right reachable set $R_p^{rt}(\mathbf{p}_0, \bar{t})$ ($R_e^{rt}(\mathbf{e}_0, \bar{t})$) is a continuous subset for all $t \geq 2\pi \frac{r_p}{v_{pm}}$ ($t \geq 2\pi \frac{r_e}{v_{em}}$).

Definition 36. Blocking set $B_p(\mathbf{p}_0, \mathbf{e}_0, \bar{t})$: Consider Figure 7.1 and $\bar{t} \geq 2\pi r_p/v_{pm}$. Construct a line segment EP , joining the initial position of the evader (E) to the initial position of the pursuer (P). Draw tangents to the pursuer circles parallel to EP directed from the evader to pursuer. Let the tangents be called $T_l^1, T_l^2, T_r^1, T_r^2$. Only one tangent in the pair $\{T_l^1, T_l^2\}$ has same orientation as the left pursuer circle and we denote it by T_l^v . Let \tilde{T}_l^v be the curve obtained by concatenation of the arc PA and T_l^v as shown in Figure 7.2. Similarly, the tangent in $\{T_r^1, T_r^2\}$, having same orientation as the right pursuer circle, will be denoted by T_r^v . Also, let \tilde{T}_r^v be the curve obtained by concatenation of the arc PC and T_r^v as shown in Figure 7.2. The curves \tilde{T}_l^v is the curve of type LS while \tilde{T}_r^v is the curve of type RS up to the time \bar{t} . Hence, \tilde{T}_r^v ends at point D while \tilde{T}_l^v ends at point B . The portion of $R_p(\mathbf{p}_0, \bar{t})$ shaded by sloped lines between \tilde{T}_l^v and \tilde{T}_r^v , containing the initial position of the evader (marked by E in Figure 7.2), is defined to be the blocking set $B_p(\mathbf{p}_0, \mathbf{e}_0, \bar{t})$.

The shaded region in Figure 7.3 shows the blocking set when evader is behind the pursuer on the right side of the pursuer. Similarly, Figure 7.7 shows the blocking set when evader is in front of the pursuer.

Lemma 37. $B_p(\mathbf{p}_0, \mathbf{e}_0, \bar{t})$ is a CSP for $\bar{t} \geq 2\pi \frac{r_e}{v_{em}}$.

Proof. It can be seen easily that any curve $\overline{\mathbf{x}\mathbf{y}}$ in $B_p(\mathbf{p}_0, \mathbf{e}_0, \bar{t})$ is a CS continuum set. Hence the claim follows. \square

Lemma 38. The union of left reachable set and right reachable set is not a continuous subset.

Proof. Consider the curve $\overline{\mathbf{x}\mathbf{y}}$ in Figure 5.2. All the trajectories of the type CS, which reach points on the segment $\overline{\mathbf{x}\mathbf{z}}$ must start on the left circle of the pursuer. Similarly, all the trajectories of the type CS which reach points on the segment $\overline{\mathbf{y}\mathbf{w}}$ must start on the right circle of the pursuer. Hence the line $\overline{\mathbf{x}\mathbf{y}}$ is not a continuum set. \square

6. CAPTURE CHARACTERIZATION USING CONTINUOUS SUBSETS

In this section we characterize the saddle point pursuit evasion trajectories under feedback using the continuous subsets of reachable sets. For this we first define the continuous safe region of the evader.

Definition 39. The *continuous safe region* $R_e^{c-}(\mathbf{e}_0, R_p^c, \bar{t})$ of a CSE $R_e^c(\mathbf{e}_0, \bar{t})$, at time \bar{t} , with respect to a CSP $R_p^c(\mathbf{p}_0, \bar{t})$ is defined as

$$\begin{aligned}
 R_e^{c-}(\mathbf{e}_0, R_p^c, \bar{t}) &= \{ \mathbf{z} \in \mathbb{R}^2 : \mathbf{z} \in R_e^c(\mathbf{e}_0, \bar{t}) \setminus R_p^c(\mathbf{p}_0, \bar{t}) \\
 &\quad \text{and } \exists \text{ an evader trajectory with} \\
 &\quad \mathbf{e}_{|\mathbb{R}^2}(t_1) = \mathbf{z} \text{ for some} \\
 &\quad t_1 \leq \bar{t} \text{ and } \mathbf{e}_{|\mathbb{R}^2}(t) \notin R_p^c(\mathbf{p}_0, t) \\
 &\quad \text{at each } t \leq t_1 \}
 \end{aligned}$$

The collection of all the CSP (CSE) at time \bar{t} from initial position \mathbf{p}_0 (\mathbf{e}_0) is denoted by $\mathfrak{R}_p(\mathbf{p}_0, \bar{t})$ ($\mathfrak{R}_e(\mathbf{e}_0, \bar{t})$).

$$\begin{aligned}
 \mathfrak{R}_e(\mathbf{e}_0, \bar{t}) &= \{ R_e^c(\mathbf{e}_0, \bar{t}) : R_e^c(\mathbf{e}_0, \bar{t}) \subseteq R_e(\mathbf{e}_0, \bar{t}) \} \\
 \mathfrak{R}_p(\mathbf{p}_0, \bar{t}) &= \{ R_p^c(\mathbf{p}_0, \bar{t}) : R_p^c(\mathbf{p}_0, \bar{t}) \subseteq R_p(\mathbf{p}_0, \bar{t}) \}
 \end{aligned}$$

In the next theorems, we characterize the point of capture in terms of continuous subsets of reachable sets. Let

$$(6.1) \quad T := \inf\{t \in \mathbb{R} : \forall R_e^c(\mathbf{e}_0, t) \in \mathfrak{R}_e(\mathbf{e}_0, t) \\ \exists R_p^c(\mathbf{p}_0, t) \in \mathfrak{R}_p(\mathbf{p}_0, t) \text{ s.t. } R_e^{c-}(\mathbf{e}_0, R_p^c, t) = \emptyset\}$$

We show next that $T = T^*$, where T^* is min – max time to capture as defined in Definition 4.

Definition 40. Continuous containment: If the continuous safe region of a CSE $R_e^c(\mathbf{e}_0, \bar{t})$, at time \bar{t} , with respect to CSP $R_p^c(\mathbf{p}_0, \bar{t})$ be such that $R_e^{c-}(\mathbf{e}_0, R_p^c, \bar{t}) = \emptyset$, then we say that $R_p^c(\mathbf{p}_0, \bar{t})$ contains $R_e^c(\mathbf{e}_0, \bar{t})$ continuously.

Theorem 41. *Let T be as given by (6.1). For every trajectory \mathbf{e} of the evader corresponding to feedback policy $\mathbf{u}_e \in \mathcal{U}_e$ there exists a pursuer trajectory corresponding to feedback strategy $\mathbf{u}_p \in \mathcal{U}_p$ s.t. $\mathbf{e}_{|\mathbb{R}^2}(t) = \mathbf{p}_{|\mathbb{R}^2}(t)$ for some $t \leq T$.*

Proof. Since, for all $R_e^c(\mathbf{e}_0, T) \in \mathfrak{R}_e(\mathbf{e}_0, T)$, there exists an $R_p^c(\mathbf{p}_0, T) \in \mathfrak{R}_p(\mathbf{p}_0, T)$ s.t. $R_e^{c-}(\mathbf{e}_0, R_p^c, T) = \emptyset$, regardless of the input strategy $\mathbf{u}_e \in \mathcal{U}_e$ that the evader selects, there exists an open-loop pursuer strategy $\mathbf{u}_p \in \mathcal{U}_p$ such that the evader will be captured at a point say $\mathbf{c} \in \mathbb{R}^2$. However, if the evader is allowed feedback policies, it can execute deviations about \mathbf{u}_e continuously by using the correct information about the pursuit trajectory \mathbf{p} chosen by the pursuer. Let the evader input deviate by $\delta \mathbf{u}_e$ and the evader trajectory by $\delta \mathbf{e}$. Let the new evader trajectory $\mathbf{e}' = \mathbf{e} + \delta \mathbf{e}$ be such that $\mathbf{e}'_{|\mathbb{R}^2}(T) = \mathbf{c}' \in \mathbb{R}^2$. Let $\overline{\mathbf{c}\mathbf{c}'}$ be any curve between points \mathbf{c} and \mathbf{c}' such that $\overline{\mathbf{c}\mathbf{c}'} \in R_e^c(\mathbf{e}_0, T)$ for some CSE $R_e^c(\mathbf{e}_0, T)$. Since the curve $\overline{\mathbf{c}\mathbf{c}'}$ is in some CSE $R_e^c(\mathbf{e}_0, T)$, and $R_e^{c-}(\mathbf{e}_0, R_p^c, T) = \emptyset$ we have $\overline{\mathbf{c}\mathbf{c}'} \in R_p^c(\mathbf{p}_0, T)$ for some CSP $R_p^c(\mathbf{p}_0, T)$. Thus, there exists a pursuer input $\mathbf{u}'_p = \mathbf{u}_p + \delta \mathbf{u}_p$ such that the $\mathbf{p}'_{|\mathbb{R}^2}(T) = \mathbf{c}'$ for the trajectory \mathbf{p}' corresponding to the input \mathbf{u}'_p and some time $t \leq T$. \square

This proves that there exists a feedback policy for pursuer which leads to capture in time $t \leq T$ irrespective of the evasion policy chosen by the evader. Next we show that there exists an evasion policy which can ensure that even with the best pursuit policy, capture happens only at T and no sooner.

Definition 42. Let $\mathcal{L}_e(\mathbf{e}_0, T)$ be a CSE. Let $\mathcal{L}_e^-(\mathbf{e}_0, R_p^c, T - \delta) \neq \emptyset$ for all $\delta > 0$ and for all $R_p^c(\mathbf{p}_0, T - \delta) \in \mathfrak{R}_p$. Let $\mathcal{C}_p(\mathbf{p}_0, T)$ be a CSP such that $\mathcal{L}_e^-(\mathbf{e}_0, \mathcal{C}_p, T) = \emptyset$. We call the $\mathcal{L}_e(\mathbf{e}_0, T)$ the **last CSE (LCSE)** and $\mathcal{C}_p(\mathbf{p}_0, T)$ as **capturing CSP (CCSP)**. Note that a pair of a LCSE and a CCSP is not unique.

Theorem 43. *Let T be as defined by (6.1). For every pursuer trajectory \mathbf{p} corresponding to feedback policy $\mathbf{u}_p \in \mathcal{U}_p$ there exists an evader trajectory \mathbf{e} corresponding to feedback strategy $\mathbf{u}_e \in \mathcal{U}_e$ s.t. $\mathbf{e}_{|\mathbb{R}^2}(t) \neq \mathbf{p}_{|\mathbb{R}^2}(t)$ for all $t < T$.*

Proof. This situation can be divided into two cases:

Case 1: Consider a time instant $\tilde{t} < T$ such that $\mathcal{L}_e^-(\mathbf{e}_0, R_p^c, \tilde{t}) \neq \emptyset$ for all $R_p^c(\mathbf{p}_0, \tilde{t}) \in \mathfrak{R}_p$ and $R_e^-(\mathbf{e}_0, R_p, \tilde{t}) \neq \emptyset$ for $R_p(\mathbf{p}_0, \tilde{t})$. Since $R_e^-(\mathbf{e}_0, R_p, \tilde{t}) \neq \emptyset$, there exists an evader strategy $\mathbf{u}_e \in \mathcal{U}_e$ such that $\mathbf{e}_{|\mathbb{R}^2}(t) \notin R_p(\mathbf{p}_0, t)$ for each $t \leq \tilde{t}$. Thus the evader can always escape capture at each $t \leq \tilde{t}$.

Case 2: Consider a time instant $\hat{t} < T$ such that $\mathcal{L}_e^-(\mathbf{e}_0, R_p^c, \hat{t}) \neq \emptyset$ for all $R_p^c(\mathbf{p}_0, \hat{t}) \in \mathfrak{R}_p$ but $R_e^-(\mathbf{e}_0, R_p, \hat{t}) = \emptyset$. Since $R_e^-(\mathbf{e}_0, R_p, \hat{t}) = \emptyset$, every trajectory \mathbf{e} of the evader, corresponding to open loop input \mathbf{u}_e , can be intercepted by some pursuer strategy \mathbf{p} corresponding to a suitable pursuer input \mathbf{u}_p . This is shown in Figure 6.1 where the solid curve (labeled \mathbf{e}) denotes an evader trajectory $\mathbf{e}_{|\mathbb{R}^2}$ and the solid curve (labeled \mathbf{p}) denotes the pursuer trajectory $\mathbf{p}_{|\mathbb{R}^2}$. Let the pursuer strategy \mathbf{p} intercept the evader, using the input \mathbf{u}_e , at a point $\mathbf{c} \in \mathcal{L}_e(\mathbf{e}_0, \hat{t})$. Since, $\mathcal{L}_e^-(\mathbf{e}_0, R_p^c, \hat{t}) \neq \emptyset \forall R_p^c(\mathbf{p}_0, \hat{t}) \in \mathfrak{R}_p$, \exists a curve $\overline{\mathbf{x}\mathbf{y}} \in \mathcal{L}_e(\mathbf{e}_0, \hat{t})$ (depicted by the solid curve from \mathbf{x} to \mathbf{y} in Figure 6.1) which is not a continuum set for the pursuer. Extend the

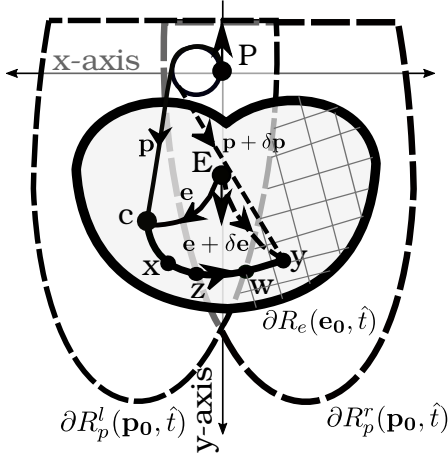


FIGURE 6.1. Only Containment: Pursuer cannot follow all the variations of the evader

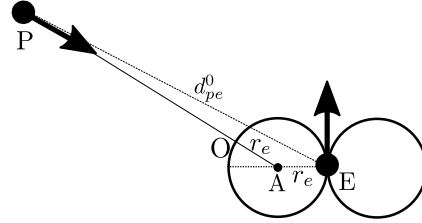


FIGURE 6.2. Evader capture after $t \geq 2\pi r_e / v_{e_m}$

curve \overline{xy} from point x to $c \in \mathcal{L}_e(\mathbf{e}_0, \hat{t})$ by a curve $\overline{xc} \in \mathcal{L}_e(\mathbf{e}_0, \hat{t})$. Call the new curve \overline{cy} . Since the curve $\overline{xy} \in \mathcal{L}_e^-(\mathbf{e}_0, R_p^c, \hat{t})$ is not a continuum set for the pursuer, the curve \overline{cy} is also not a continuum set for the pursuer. However, the curve $\overline{cy} \in \mathcal{L}_e^-(\mathbf{e}_0, R_p^c, \hat{t})$ is a continuum set for the evader. Thus the evader with a variation $\delta \mathbf{u}_e$ in its strategy can change the end point to y from point c (The evader trajectory corresponding to input $\mathbf{u}_e + \delta \mathbf{u}_e$ is shown by a dashed curve and labeled $e + \delta e$). However, since \overline{cy} is not a continuum set for the pursuer, the pursuer cannot catch the evader in time \hat{t} using an admissible variation $\delta \mathbf{u}_p$. Thus the evader can always avoid capture for all time $t \leq \hat{t} < T$. \square

Theorem 44. T is the min – max time to capture i.e. $T = T^*$ (recall Definition 4).

Proof. By Theorem 43, in order to maximize the time-to-capture the evader should use input strategy $\mathbf{u}_e^* \in \mathcal{U}_e$ such that, $\mathbf{e}_{|\mathbb{R}^2}(T) = \mathbf{z} \in \mathcal{L}_e(\mathbf{e}_0, T)$, and $\mathbf{e}_{|\mathbb{R}^2}(t) \notin \mathcal{C}_p(\mathbf{p}_0, t) \forall t < T$. On the other hand, the pursuer should use time-optimal input strategy $\mathbf{u}_p^* \in \mathcal{U}_p$ such that $\mathbf{p}_{|\mathbb{R}^2}(T) = \mathbf{z}$ and $\mathbf{p}_{|\mathbb{R}^2}(t) \in \mathcal{C}_p(\mathbf{p}_0, T) \forall t \leq T$ in order to minimize the time to capture the evader. Thus if the evader uses $\mathbf{u}_e^* \in \mathcal{U}_e$ and pursuer uses $\mathbf{u}_p^* \in \mathcal{U}_p$ the time to capture $T_c(\mathbf{u}_p^*, \mathbf{u}_e^*) = T$. If the evader deviates from \mathbf{u}_e^* by $\delta \mathbf{u}_e$ then by Theorem 41 it will be captured at $T_c(\mathbf{u}_p^*, \mathbf{u}_e^* + \delta \mathbf{u}_e) \leq T$. Similarly, if the pursuer deviates from \mathbf{u}_p^* by $\delta \mathbf{u}_p$ it will not be able to reach point $\mathbf{e}_{|\mathbb{R}^2}(T) = \mathbf{z} \in \mathcal{C}_p(\mathbf{e}_0, T)$ at time T and we have $T \leq T_c(\mathbf{u}_p^* + \delta \mathbf{u}_p, \mathbf{u}_e^*)$. Thus,

$$(6.2) \quad T_c(\mathbf{u}_p^*, \mathbf{u}_e^* + \delta \mathbf{u}_e) \leq T = T_c(\mathbf{u}_p^*, \mathbf{u}_e^*) \leq T_c(\mathbf{u}_p^* + \delta \mathbf{u}_p, \mathbf{u}_e^*)$$

and hence \mathbf{u}_e^* and \mathbf{u}_p^* are the feedback saddle-point strategies. Since, T satisfies (6.2) we have $T = T^*$. \square

7. ANALYSIS OF GAME OF TWO CARS USING CONTINUOUS SUBSETS

In this section we explicitly characterize the continuous subset of evader's reachable set which will be the *LCSE*. For the pursuer we show that *CCSP* will be a set from among three particular continuous subsets of the pursuer's reachable set. Using *LCSE* and *CCSP* we show that the saddle point trajectories are of the type *CS*.

7.1. Characterization of LCSE. In this section we characterize the LCSE $\mathcal{L}_e(\mathbf{e}_0, T^*)$. Recall that r_p and r_e are the minimum turning radii of the pursuer and the evader respectively, while d_{pe}^0 denotes the initial distance between the pursuer and the evader. If the capture time $T^* \geq 2\pi r_e/v_{em}$, then we show that the boundary of LCSE is the external boundary of evader's reachable set. This simplifies the analysis of the game significantly. Hence, in order to ensure that the capture of evader takes at least time $2\pi r_e/v_{em}$ we add an assumption on the initial distance between the pursuer and the evader.

Lemma 45. *If $d_{pe}^0 \geq 2r_e + 2\pi r_e(v_{pm}/v_{em})$ then capture can occur only at time $t \geq 2\pi r_e/v_{em}$.*

Proof. Let the evader be located at E , at a distance d_{pe}^0 away from the pursuer located at P , as shown in Figure 6.2. Let PA be the line from pursuer's position to the center of anti-clockwise evader circle denoted by point A . Also, let PA intersect the anticlockwise circle at point O . The least time for the pursuer to reach point O is

$$(7.1) \quad \begin{aligned} t_m &:= \text{len}(PO)/v_{pm} \\ &= (\text{len}(PA) - r_e)/v_{pm} \end{aligned}$$

Also from triangle inequality we have $\text{len}(PA) \geq \text{len}(PE) - r_e$. Thus (7.1) becomes

$$\begin{aligned} t_m &\geq (\text{len}(PE) - r_e - r_e)/v_{pm} \\ &= [d_{pe}^0 - 2r_e]/v_{pm} \end{aligned}$$

Let, $t_p := (d_{pe}^0 - 2r_e)/v_{pm}$ and $t_e := 2\pi r_e/v_{em}$. Thus if $t_p \geq t_e$ the pursuer requires at least t_e time to reach any point on evader circles. Thus the evader, by using $v_e(t) = 0$ and $u_e(t) = 0 \forall t$ can avoid capture up to time t_e (since it remains at point $E \forall t$ and pursuer takes at least time t_e to reach it). Further, if it uses time optimal evasion strategy then the time to capture will certainly be greater than t_e . Thus, if $d_{pe}^0 \geq 2r_e + 2\pi r_e(v_{pm}/v_{em})$ we have $t_p = (d_{pe}^0 - 2r_e)/v_{pm} \geq 2\pi r_e/v_{em}$. This implies $t_p \geq t_e$ and the claim follows. \square

Recall that, by Lemma 32, the central reachable set $R_e^{CR}(\mathbf{e}_0, T^*)$ is a CSE. In next theorem we prove that the LCSE is in fact $R_e^{CR}(\mathbf{e}_0, T^*)$ if $d_{pe}^0 \geq 2r_e + 2\pi r_e(v_{pm}/v_{em})$. Further, since the boundary of $R_e^{CR}(\mathbf{e}_0, T^*)$ and the external boundary of $R_e(\mathbf{e}_0, T^*)$ are the same, it follows that the whole reachable set of the evader must be contained in some continuous subset of the evader's reachable set. In the next theorem we specialize the Theorems 41 and 43 for the assumption that $d_{pe}^0 \geq 2r_e + 2\pi r_e(v_{pm}/v_{em})$, and give a necessary and sufficient condition for capture under feedback trajectories.

Theorem 46. *Let $d_{pe}^0 \geq 2r_e + 2\pi r_e(v_{pm}/v_{em})$. For every evader trajectory $\mathbf{e}_{|\mathbb{R}^2}$ generated by feedback policy $\mathbf{u}_e \in \mathcal{U}$ there exists a pursuer trajectory $\mathbf{p}_{|\mathbb{R}^2}$ corresponding to feedback strategy $\mathbf{u}_p \in \mathcal{U}_p$ s.t. $\mathbf{e}_{|\mathbb{R}^2}(t) = \mathbf{p}_{|\mathbb{R}^2}(t)$ for some $t \leq T^*$ if and only if $R_e^-(\mathbf{e}_0, \mathcal{C}_p, T^*) = \emptyset$ for a CCSP $\mathcal{C}_p(\mathbf{p}_0, T^*)$.*

Proof. First we show the *only if* part. As seen in Lemma 45, if $d_{pe}^0 \geq 2r_e + 2\pi r_e(v_{pm}/v_{em})$ the pursuer can capture the evader only after time $t_e = 2\pi r_e/v_{em}$. The evader's central reachable set after time $t \geq t_e = 2\pi r_e/v_{em}$ is shown in Figure 5.3. It can be easily seen that the external boundary of the evader's reachable set and that of the central reachable set are the same i.e. $\partial R_e(\mathbf{e}_0, T^*) = \partial R_e^{CR}(\mathbf{e}_0, T^*)$. Now, $R_e^{CR}(\mathbf{e}_0, T^*)$ is a CSE. By Theorems 43 and 41 $R_e^{CR}(\mathbf{e}_0, T^*)$ must be contained inside some CCSP $\mathcal{C}_p(\mathbf{p}_0, T^*)$ for capture to occur at time $t \leq T^*$. Since, $\partial R_e(\mathbf{e}_0, T^*) = \partial R_e^{CR}(\mathbf{e}_0, T^*)$, it is necessary that $R_e(\mathbf{e}_0, T^*)$ must be contained inside some $\mathcal{C}_p(\mathbf{p}_0, T^*)$ for the capture to occur at $t \leq T^*$.

Now we prove the *if* part. Since $R_e^c(\mathbf{e}_0, T^*) \subseteq R_e(\mathbf{e}_0, T^*)$ for all $R_e^c(\mathbf{e}_0, T^*) \in \mathfrak{R}(\mathbf{e}_0, T^*)$, the condition $R_e^-(\mathbf{e}_0, \mathcal{C}_p, T^*) = \emptyset$ implies that every $R_e^c(\mathbf{e}_0, T^*) \in \mathfrak{R}(\mathbf{e}_0, T^*)$ is such that $R_e^{c-}(\mathbf{e}_0, \mathcal{C}_p, T^*) = \emptyset$ for some corresponding CCSP $\mathcal{C}_p(\mathbf{p}_0, T^*)$. Thus by Theorems 41 and 43 we can conclude that capture will occur at $t \leq T^*$. \square

7.2. Characterization of CCSP. Next, we will characterize $CCSP \mathcal{C}_p(\mathbf{p}_0, T^*)$ in order to determine the nature of feedback strategies. We will show that the $CCSP$ is either the blocking set $B_p(\mathbf{p}_0, \mathbf{e}_0, T^*)$ or the truncated left reachable set $R_p^{l_t}(\mathbf{p}_0, T^*)$ or the truncated right reachable set $R_p^{r_t}(\mathbf{p}_0, T^*)$. First we define the concept of blocking LS and RS trajectories of the pursuer.

Definition 47. Blocking trajectory of the pursuer : If the initial position of the evader (\mathbf{e}_0) and pursuer (\mathbf{p}_0) is such that all the points on a pursuer trajectory are reached by the pursuer earlier than the evader then we say that such a trajectory is a blocking trajectory. Further, if the blocking trajectory is of the type LS (RS) then we call it LS (RS) blocking trajectory.

This concept of blocking trajectory will be used to analyze the containment of evader's reachable set by $B_p(\mathbf{p}_0, \mathbf{e}_0, T^*)$, $R_p^{l_t}(\mathbf{p}_0, T^*)$, and $R_p^{r_t}(\mathbf{p}_0, T^*)$.

Continuous capture by blocking set. We show that the blocking set (defined in Definition 36 and shown to be a continuous subset in Lemma 37) will contain the evader's reachable set for all initial conditions of the pursuer and the evader such that $d_{pe}^0 \geq 2r_e + 2\pi r_e(v_{p_m}/v_{e_m})$. Recall that \tilde{T}_l^v and \tilde{T}_r^v are the trajectories of the type LS and RS as defined in Definition 36. The next lemma follows easily from the construction of $B_p(\mathbf{p}_0, \mathbf{e}_0, \bar{t})$ for some time $\bar{t} \geq 2\pi r_p/v_{p_m}$.

Lemma 48. \tilde{T}_l^v is a blocking LS trajectory while \tilde{T}_r^v is a blocking RS trajectory if $d_{pe}^0 \geq 2r_e + 2\pi r_e(v_{p_m}/v_{e_m})$.

Remark 49. By Lemma 48, \tilde{T}_l^v and \tilde{T}_r^v block the evader from entering the region shown by crisscross shading in Figure 7.2. Some examples of blocking sets have been shown in Figures 7.3, 7.7, and 7.6. As can be seen from these examples, at most one curve out of \tilde{T}_l^v and \tilde{T}_r^v can end on the left internal boundary or the right internal boundary for any position of the pursuer and evader after time $\bar{t} \geq 2\pi r_p/v_{p_m}$.

Next we show that for all possible initial positions of the evader, the blocking set will contain the evader's reachable set at some time $T_b < \infty$.

Lemma 50. For every evader and pursuer initial positions such that $d_{pe}^0 \geq 2r_e + 2\pi r_e(v_{p_m}/v_{e_m})$, the set $R_e^-(\mathbf{e}_0, B_p, T_b) = \emptyset$ for some time $T_b < \infty$.

Proof. Recall that, if $d_{pe}^0 \geq 2r_e + 2\pi r_e(v_{p_m}/v_{e_m})$ then each of the left reachable set and the right reachable set contain the evader's reachable set at times T_l and T_r respectively (by Lemma 17 and Lemma 18). Now, since either the blocking curve \tilde{T}_l^v or the blocking curve \tilde{T}_r^v may end on the internal boundary, without loss of generality, let \tilde{T}_l^v end on the left internal boundary (see Definition 14) as shown in Figure 7.1. Now consider the left reachable set of the pursuer. Some portion of the left reachable set is not a part of the blocking set. Thus, at time $t_m = \max(T_l, T_r)$, $B_p(\mathbf{p}_0, \mathbf{e}_0, t_m)$ may not contain some part of $R_e(\mathbf{e}_0, t_m)$ even if the left reachable set contains the reachable set completely. However, since $d_{pe}^0 \geq 2r_e + 2\pi r_e(v_{p_m}/v_{e_m})$ the evader cannot enter this part as \tilde{T}_l^v and \tilde{T}_r^v are blocking curves (by Lemma 48). Apart from this portion the left reachable set is a part of $B_p(\mathbf{p}_0, \mathbf{e}_0, t_m)$. Thus, the remaining part of $R_e(\mathbf{e}_0, t_m)$ is contained in the blocking set and we have $R_e^-(\mathbf{e}_0, B_p, t_m) = \emptyset$. Hence, for some time $T_b \leq t_m$ we will have $R_e^-(\mathbf{e}_0, B_p, T_b) = \emptyset$. \square

Continuous containment by truncated left reachable set. In this section we analyze the conditions under which $R_p^{l_t}(\mathbf{p}_0, \bar{t})$ and $R_p^{r_t}(\mathbf{p}_0, \bar{t})$ can contain the evader's reachable set at some time \bar{t} . First we define two LS (RS) blocking trajectories for the truncated left (right) reachable set.

Let PA be the curve defined by (3.1) with $t_1 = 0$ and is shown in Figure 3.2. We call this curve BL^1 . Similarly, let PCB be the curve defined by (3.1) with $t_1 = 2\pi r_p/v_{p_m}$ and is shown in Figure 3.2. We call this curve BL^2 . Analogously, BR^1 and BR^2 are defined for the truncated right reachable set.

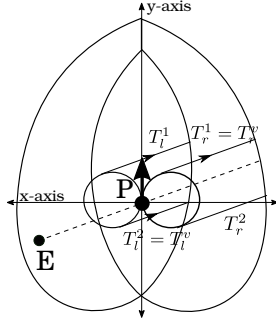


FIGURE 7.1. Construction of $B_p(\mathbf{p}_0, \mathbf{e}_0, \bar{t})$

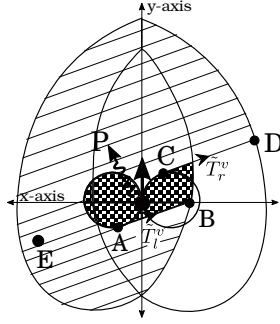


FIGURE 7.2. $B_p(\mathbf{p}_0, \mathbf{e}_0, \bar{t})$: Evader behind on left side (shaded region)

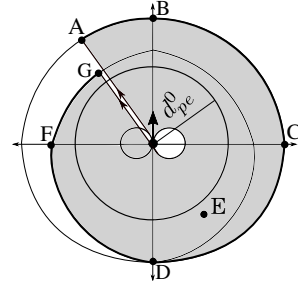


FIGURE 7.3. $B_p(\mathbf{p}_0, \mathbf{e}_0, \bar{t})$: Evader behind on right side (shaded region)

Remark 51. Now, the left reachable set $R_p^l(\mathbf{p}_0, T_l)$ contains the evader’s reachable set at time T_l (by Lemma 17). Since the truncated reachable set does not contain PA and the anti-clockwise circle $A_p(0)$, hence if evader’s reachable set intersects the line PA or the anti-clockwise circle, continuous containment by $R_p^l(\mathbf{p}_0, T_l)$ will not happen. However, such a situation is avoided since BL^1 and BL^2 act as blocking curves for some initial conditions of the pursuer and the evader, and block the evader from entering the points in PA and $A_p(0)$ analogous to what \tilde{T}_l^v and \tilde{T}_r^v achieve for the blocking set. This is shown in Proposition 57.

First we define some terminology. Consider Figure 7.4. Let OPQ be the line passing through the pursuer position P and perpendicular to the orientation of the pursuer. If the evader is in the closed half plane in the direction opposite to the orientation of the pursuer then we say that the evader is behind the pursuer. If the evader is located in the open half plane in the direction of the orientation of the pursuer then we say that the evader is located in the front of the pursuer. For $R_p^l(\mathbf{p}_0, T_l)$, let PF be the line as shown in Figure 7.4 at an angle θ with respect to PS . The shaded region between PO and PF , for $\theta = \arccos(2\pi r_p v_{e_m} / (v_{p_m} d_{pe}^0))$, is denoted by $S^l(T_l)$. Similarly, for $R_p^{r_t}(\mathbf{p}_0, T_r)$ let PF be the line as shown in Figure 7.5 at an angle θ with respect to PS . The shaded region between PO and PF for, $\theta = \arccos(2\pi r_p v_{e_m} / (v_{p_m} d_{pe}^0))$, is denoted by $S^r(T_r)$.

Lemma 52. Let $d_{pe}^0 \geq 2r_e + 2\pi r_e(v_{p_m}/v_{e_m})$ and let the evader’s initial position be in $S^l(T_l)$. Then, $R_p^l(\mathbf{p}_0, T_l)$ will contain the evader’s reachable set continuously.

Proof. BL^1 as blocking trajectory : Since evader is in $S^l(T_l)$, it is behind the pursuer. All the points on the trajectory BL^1 can be reached by the pursuer before the evader can reach them. Hence, it becomes the blocking LS trajectory. Thus BL^1 will prevent the evader from reaching any point on PA from the left side of the pursuer.

BL^2 as blocking trajectory : If $d_{pe}^0 \geq 2r_e + 2\pi r_e(v_{p_m}/v_{e_m})$ then the pursuer can reach all the points on the anti-clockwise circle of the pursuer before the evader (See Lemma 81 in appendix for details). Since the boundary of $A_p(0)$ forms a part of BL^2 we can conclude that BL^2 prevents the evader from entering $A_p(0)$.

Now, if the evader tries to reach any point on line PA from the right, while the pursuer is initially traveling on $A_p(0)$, we will show that BL^2 will intercept the evader. If the pursuer follows BL^2 , it will reach point

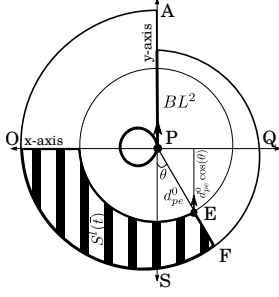


FIGURE
7.4. BL^2 :
Blocking LS
trajectory

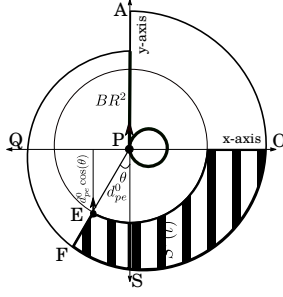


FIGURE
7.5. BR^2 :
Blocking RS
trajectory

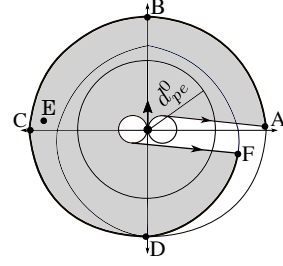


FIGURE
7.6. $B_p(\mathbf{p}_0, \mathbf{e}_0, T_b)$
as active set

P again after encircling the anticlockwise circle once, for which it will require time $t_p := 2\pi r_p/v_{p_m}$. Thus if the evader requires time $t_e \geq t_p$ to reach the line OPQ then BL^2 will be a blocking LS trajectory. Let the evader be located at an angle θ with respect to line PS as shown in Figure 7.4. At this position the evader requires minimum time to reach a point on line OPQ if it is pointing upwards. This minimum time is $d_{pe}^0 \cos(\theta)/v_{e_m}$. Thus $t_e \geq d_{pe}^0 \cos(\theta)/v_{e_m}$. Hence BL^2 is the blocking trajectory if

$$\begin{aligned} d_{pe}^0 \cos(\theta)/v_{e_m} &\geq 2\pi r_p/v_{p_m} \\ \cos(\theta) &\geq 2\pi r_p v_{e_m}/(v_{p_m} d_{pe}^0) \end{aligned}$$

This implies that for $\theta \leq \arccos(2\pi r_p v_{e_m}/(v_{p_m} d_{pe}^0))$, BL^2 will act as blocking trajectory.

The left reachable set contains the evader's reachable set at time T_l (by Lemma 17). Further, BL^1 and BL^2 act as blocking curves and block the evader from entering the points in PA and $A_p(0)$ and the claim follows. \square

Definition 53. Let T_l^c be the minimum time s.t. $R_e(\mathbf{e}_0, T_l^c) \subseteq R_p^{l_t}(\mathbf{p}_0, T_l^c)$ continuously i.e. $R_e^-(\mathbf{e}_0, R_p^{l_t}, T_l^c) = \emptyset$. If for some initial positions of the pursuer and the evader, $R_p^{l_t}(\mathbf{p}_0, T_l^c)$ does not contain $R_e(\mathbf{e}_0, T_l^c)$ continuously then we say $R_e^-(\mathbf{e}_0, R_p^{l_t}, T_l^c) = \emptyset$ at $T_l^c = \infty$.

Remark 54. From the above analysis it follows that if $T_l^c < \infty$ then $T_l^c = T_l$. However, if $T_l^c = \infty$ this implies that the truncated left reachable set cannot contain evader's reachable set continuously.

Lemma 55. Let $d_{pe}^0 \geq 2r_e + 2\pi r_e(v_{p_m}/v_{e_m})$ and let the evader's initial position be located in $S^r(T_r)$. Then, $R_p^{r_t}(\mathbf{p}_0, T_r)$ will contain the evader's reachable set continuously at some finite time $\bar{t} \geq 2\pi r_p/v_{p_m}$.

Remark 56. The minimum time for continuous containment by the truncated right reachable set is denoted by T_r^c . If $T_r^c < \infty$ then $T_r^c = T_r$. However, if $T_r^c = \infty$ this implies that the truncated right reachable set cannot contain evader's reachable set continuously.

Proposition 57. Let $d_{pe}^0 \geq 2r_e + 2\pi r_e(v_{p_m}/v_{e_m})$. If the evader is behind the pursuer then the evader's reachable set is contained continuously in the left reachable set or the right reachable set or both at time $t_{lr} = \min(T_l^c, T_r^c)$.

Proof. If the evader is behind the pursuer at a distance greater than $d_{pe}^0 \geq 2r_e + 2\pi r_e(v_{p_m}/v_{e_m})$ it is either located in $S^l(T_l^c)$ or $S^r(T_r^c)$ or both and the claim follows from Lemma 52 and Lemma 55. \square

Representative set and frontier boundaries. Next, we define the representative set at time $t \geq 2\pi r_p/v_{p_m}$ which comprises of the blocking set, truncated left reachable set, and the truncated right reachable set.

Definition 58. *Representative set* at time $t \geq 2\pi r_p/v_{p_m}$ is

$$\mathfrak{R}(\mathbf{p}_0, \mathbf{e}_0, t) : = \{B_p(\mathbf{p}_0, \mathbf{e}_0, t), R_p^{l_t}(\mathbf{p}_0, t), R_p^{r_t}(\mathbf{p}_0, t)\}$$

Definition 59. Let T_a be the time such that for some $\tilde{R}_p^c \in \mathfrak{R}(\mathbf{p}_0, \mathbf{e}_0, T_a)$ we have $R_e^-(\mathbf{e}_0, \tilde{R}_p^c, T_a) = \emptyset$ and for all $t < T_a$, $R_e^-(\mathbf{e}_0, R_p^c, t) \neq \emptyset$ for all $R_p^c \in \mathfrak{R}(\mathbf{p}_0, \mathbf{e}_0, t)$ i.e. $T_a = \min\{T_b, T_l^c, T_r^c\}$. We denote this set $\tilde{R}_p^c \in \mathfrak{R}(\mathbf{p}_0, \mathbf{e}_0, T_a)$ by $\mathcal{A}_p(T_a)$ and call it the *active pursuer set*.

Note that, since $R_e^-(\mathbf{e}_0, B_p, T_b) = \emptyset$ for some time $T_b < \infty$ (Lemma 50), we have $T_a < \infty$.

Remark 60. The capture criterion, which could not be explained using only containment of reachable sets can now be explained using the active set and *LCSE*. Consider the position of the pursuer and evader as shown in the Figure 4.1. In this case the active set is the left reachable set as shown in Figure 7.11 and capture occurs at time $T_l^c = T_l$. Further, at time $t < T_l$, the safe region of evader is non-empty (shown in Figure 7.12). Next consider the situation when the evader is located ahead of the pursuer as shown in Figure 4.3. In this case the blocking set is the active set. The capture is shown in Figure 7.8 and occurs at time T_b . For any time $t < T_b$ the safe region of the evader is non-empty (as shown in Figure 7.9) and the evader can escape capture using feedback strategies. In the above examples the active set explains capture under feedback strategies. In fact, we will show that if the evader is in front of the pursuer then it suffices to consider blocking set as *CCSP* and if the evader is behind the pursuer then it suffices to consider either the left reachable set or the right reachable set as *CCSP*.

Next we define frontier boundary for all the sets in the representative set.

Definition 61. *Frontier boundary:*

- (1) The *frontier boundary of $R_p^{l_t}(\mathbf{p}_0, t)$* is the portion of the external boundary denoted by *ADEFB* (start point *A* to end point *B*) as shown in Figure 3.2 by dashed curve i.e. we exclude the portion *BA* from $\partial R_p^{l_t}(\mathbf{p}_0, t)$.
- (2) The *frontier boundary of $R_p^{r_t}(\mathbf{p}_0, t)$* is defined analogously.
- (3) The *frontier boundary of the blocking set* is the portion of external boundary of the blocking set excluding the blocking curves \tilde{T}_l^v and \tilde{T}_r^v . For example, the frontier boundary of blocking set in Figure 7.3 is denoted by *ABCDGF*.

Remark 62. The frontier boundaries of all the sets expand outwards radially with time. Also the external boundary of the evader reachable set expands out radially. As a result, for the active set, the capture occurs on the frontier boundary.

Next we demonstrate that if $d_{pe}^0 \geq 2r_e + 2\pi r_e(v_{p_m}/v_{e_m})$ the evader can always escape capture for all time $t < T_a$. We do this in by considering a particular set in representative set to be a active set in the Propositions 63, 64, and 68.

Proposition 63. *Let $d_{pe}^0 \geq 2r_e + 2\pi r_e(v_{p_m}/v_{e_m})$. If $\mathcal{A}_p(T_a) = R_p^{l_t}(\mathbf{p}_0, T_a)$ and $T_a = T_l^c < \infty$, then the evader can always escape capture for $t < T_a$ by using feedback strategy.*

Proof. First we divide the frontier boundary of $R_p^{l_t}(\mathbf{p}_0, T_a)$ into two parts *ADE* and *EGFHB* as shown in Figure 7.10. Let $\mathbf{z} \in \mathbb{R}^2$ be a last point of $R_e(\mathbf{e}_0, T_a)$ covered by $R_p^{l_t}(\mathbf{p}_0, T_a)$ at time T_a . Since the frontier boundary of $R_p^{l_t}(\mathbf{p}_0, t)$ and the external boundary $R_e(\mathbf{e}_0, t)$ both grow out radially with time t , \mathbf{z} will lie on

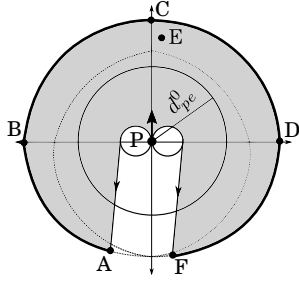


FIGURE 7.7. $B_p(\mathbf{p}_0, \mathbf{e}_0, t_m)$: Evader in front (shaded region)

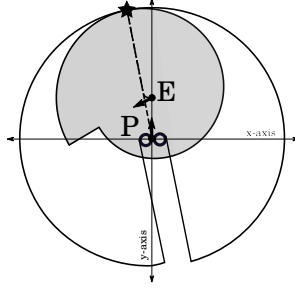


FIGURE 7.8. Active Set: Blocking set

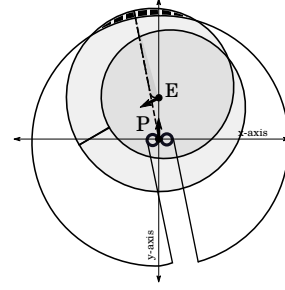


FIGURE 7.9. Evader safe region

the external boundary of $R_e(\mathbf{e}_0, T_a)$. Also, the point in $R_p^{lt}(\mathbf{p}_0, T_a)$ which covers \mathbf{z} will lie on the frontier boundary of $R_p^{lt}(\mathbf{p}_0, T_a)$. Now the situation can be divided into two cases:

Case 1: Let $\mathbf{z} \in ADE$. Then at time $T'_a < T_a$ we have $R_e^-(\mathbf{e}_0, R_p^l, T'_a) \neq \emptyset$ i.e. the pursuer's reachable set does not cover the evader's reachable set and the evader can always escape capture.

Case 2: Let $\mathbf{z} \in EGFHB$. We further divide the portion $EGFHB$ into two parts namely EGF and FHB as shown in Figure 7.10. Now let $\mathbf{z} \in FHB$. In Figure 7.10 the right reachable set is shown by dotted curve. Since $d_{pe}^0 \geq 2r_e + 2\pi r_e(v_{pm}/v_{em})$, the evader is located outside the circle of radius d_{pe}^0 . It is clear from geometry that if $\mathbf{z} \in FHB$ then the right external boundary would have covered the evader's reachable set earlier. Thus the right reachable set would have been the active set and this contradicts the assumption that $R_p^{lt}(\mathbf{p}_0, T_a)$ is the active set.

Next, let $\mathbf{z} \in EGF$. Let $T'_a < T_a$ s.t. $R_e^-(\mathbf{e}_0, R_p, T'_a) = \emptyset$ (If $R_e^-(\mathbf{e}_0, R_p, T'_a) \neq \emptyset$ then the pursuer's reachable set does not cover the evader's reachable set and the evader can always escape capture). At time T'_a , $R_p^{lt}(\mathbf{p}_0, T'_a)$ will not cover evader's reachable set completely. Since $R_e^-(\mathbf{e}_0, R_p, T'_a) = \emptyset$, this uncovered region must form a part of the right reachable set of the pursuer. Further, there must exist a point \mathbf{x} in the evader's reachable set such that $\mathbf{x} \in [R_p^{lt}(\mathbf{p}_0, T'_a)/R_p^{rt}(\mathbf{p}_0, T'_a)] \cap R_e(\mathbf{e}_0, T'_a)$. (For if such a point does not exist then the evader's reachable set at T'_a would be entirely contained by the the right reachable set. Since, $R_p^{rt}(\mathbf{p}_0, T'_a)$ is in the representative set this would contradict the assumption that $R_p^{lt}(\mathbf{p}_0, T_a)$ is the active set). Also, there exists a point $\mathbf{y} \in [R_p^{rt}(\mathbf{p}_0, T'_a)/R_p^{lt}(\mathbf{p}_0, T'_a)] \cap R_e(\mathbf{e}_0, T'_a)$ (Otherwise we would have $R_e^-(\mathbf{e}_0, R_p^l, T'_a) = \emptyset$ and this will contradict the assumption that the minimum time at which $R_e^-(\mathbf{e}_0, R_p^l, t) = \emptyset$ is T_a since $T'_a < T_a$). Now consider a curve $\overline{\mathbf{x}\mathbf{y}}$ in the evader's reachable set as shown in Figure 5.2. Since $\mathbf{z} \in EGF$, such a curve is behind the pursuer and as shown in the proof of Lemma 38 it is not a continuum curve for the pursuer. Hence, at time $T'_a < T_a$, $R_e^-(\mathbf{e}_0, R_p^c, T'_a) \neq \emptyset$ for all CSP $R_p^c(\mathbf{p}_0, T'_a)$ and the evader can escape capture. \square

The proof of Proposition 64 is similar to that of Proposition 63.

Proposition 64. Let $d_{pe}^0 \geq 2r_e + 2\pi r_e(v_{pm}/v_{em})$. If $\mathcal{A}_p(T_a) = R_p^{rt}(\mathbf{p}_0, T_a)$ and $T_a = T_r^c < \infty$, then evader can always escape capture for $t < T_a$ by using feedback strategy.

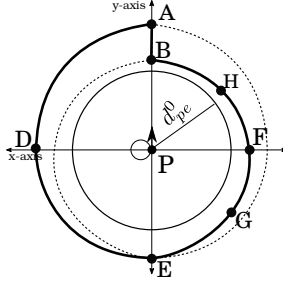


FIGURE 7.10. Left reachable set as active set

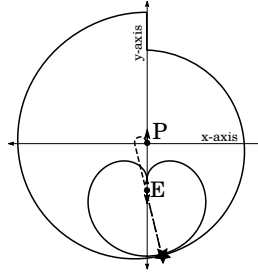


FIGURE 7.11. Continuous containment by left reachable set

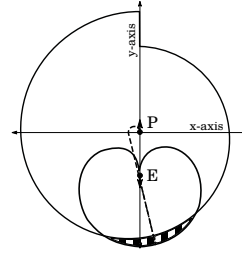


FIGURE 7.12. Safe region: Continuous containment by left reachable set

Remark 65. Consider a situation where the active set is the blocking set and either the truncated left reachable set or the truncated right reachable set contains the evader’s reachable set continuously. In such a situation either the truncated left reachable set or the truncated right reachable set is also an active set along with the blocking set. This is established in the next lemma.

Lemma 66. Let $T_{lr} = \min(T_l^c, T_r^c)$ and $d_{pe}^0 \geq 2r_e + 2\pi r_e(v_{p_m}/v_{e_m})$. If $T_{lr} < \infty$ and $B_p(\mathbf{p}_0, \mathbf{e}_0, T_b)$ is the active set such that $R_e^-(\mathbf{e}_0, B_p, T_b) = \emptyset$ then either $R_e^-(\mathbf{e}_0, R_p^l, T_b) = \emptyset$ or $R_e^-(\mathbf{p}_0, R_p^r, T_b) = \emptyset$ and $T_b = T_{lr}$.

Proof. Either the internal boundary of left reachable set or the internal boundary of the right reachable set is part of the frontier boundary of the blocking set. Without loss of generality assume that the internal boundary of the right reachable set forms a part of the frontier boundary of the blocking set as shown in Figure 7.3. Since the evader is behind the pursuer and $d_{pe}^0 \geq 2r_e + 2\pi r_e(v_{p_m}/v_{e_m})$, from Proposition 57, BR^1 and BR^2 are blocking curves. Thus the right reachable set will contain evader’s reachable set continuously. Hence, for the blocking set, the capture will occur on $BCDFG$ w.r.t Figure 7.3. The AB part of the frontier boundary is redundant. Thus the capture by right reachable set and the blocking set will be at the same point of the frontier boundary and the claim follows. \square

Note 67. Proposition 57 and Lemma 66 allow us to consider $R_p^l(\mathbf{p}_0, T_l^c)$ or $R_p^r(\mathbf{p}_0, T_r^c)$ as the active set when the evader is behind the pursuer. Also it suffices to consider only blocking set as be the active set when the evader is in the front of pursuer.

Proposition 68. Let $d_{pe}^0 \geq 2r_e + 2\pi r_e(v_{p_m}/v_{e_m})$ and let the evader be in the front of the pursuer. If $A_p(T_a) = B_p(\mathbf{p}_0, \mathbf{e}_0, T_a)$, then the evader can always escape capture for $t < T_a$ by using feedback strategy..

Proof. Consider the situation shown in Figure 7.6 where the evader (denoted by point E) is in front of the pursuer. Let \mathbf{z} be the last point of $R_e(\mathbf{e}_0, T_a)$ covered by $B_p(\mathbf{p}_0, \mathbf{e}_0, T_a)$ at time T_a . The frontier boundary of $B_p(\mathbf{p}_0, \mathbf{e}_0, t)$ and the external boundary $R_e(\mathbf{e}_0, t)$ both grow out radially with time t . Hence, the point \mathbf{z} will lie on the external boundary of $R_e(\mathbf{e}_0, T_a)$. Also, the point covering \mathbf{z} will lie on the frontier boundary of $B_p(\mathbf{p}_0, \mathbf{e}_0, T_a)$. From Figure 7.3 it is clear that $\mathbf{z} \in ABCD$. Then at time $T'_a < T_a$ we have $R_e^-(\mathbf{e}_0, B_p, T'_a) \neq \emptyset$ i.e. the pursuer’s reachable set does not cover the evader’s reachable set. This situation is shown in Figure 7.9. Thus the evader can always escape capture at time $t < T_a$. \square

The next theorem characterizes the *CCSP* and using it we determine the saddle point strategies, point of capture and time of capture in Theorem 70. Recall that T^* is the min – max time to capture under saddle-point strategies.

Theorem 69. $\mathcal{A}_p(T_a)$ is a *CCSP* and $T_a = T^*$.

Proof. Proposition 63, Proposition 64 and Proposition 68 show that the active set $\mathcal{A}_p(T_a)$ is a *CCSP*. Thus from Theorem 46 we have $T^* = T_a$. \square

Characterization of min – max trajectories.

Theorem 70. If the initial distance $d_{pe}^0 \geq 2r_e + 2\pi r_e(v_{pm}/v_{em})$, then the saddle-point strategies of the evader and the pursuer are of the type *CS* that is a circle and straight line.

Proof. Let T^* and \mathbf{z} be the time of capture and point of capture respectively if the pursuer and evader use saddle point strategies. From previous analysis, since the frontier boundaries grow out radially, the point \mathbf{z} belongs to the frontier boundary of the active set $\mathcal{A}_p(\mathbf{p}_0, T^*)$ and the external boundary of the evader’s reachable set. The time optimal trajectory for the pursuer, which lies in $\mathcal{A}_p(\mathbf{p}_0, T^*)$, to reach point \mathbf{z} is of the type *CS*. Thus, by Theorem 44, the saddle-point trajectory of the pursuer is of the type *CS*. Point \mathbf{z} also lies on the external boundary of the evader’s reachable set. The evader trajectory which reaches \mathbf{z} in minimum time is also of the type *CS*. Thus evader’s saddle-point trajectory is of the type *CS* (by Theorem 44). \square

8. HAMILTONIAN PRINCIPLE

One of the methods of computing the feedback pair $[\gamma_p^*(\mathbf{x}), \gamma_e^*(\mathbf{x})]$ is to use the Hamiltonian and Euler-Lagrange equations. As a reference for the Problems 2 and 3 we review it here briefly. Consider a system beginning at $t = 0$ given by the equation

$$\dot{\mathbf{x}}(t) = f(\mathbf{x}(t), \mathbf{u}_p(t), \mathbf{u}_e(t), t), \quad \mathbf{x}(0) = \mathbf{x}_0$$

where $\mathbf{x} : [0, t_f] \rightarrow \mathbb{R}^n$ is the state of the system and $\mathbf{u}_p(t) : [0, t_f] \rightarrow \mathbb{R}^{m_p}$ and $\mathbf{u}_e(t) : [0, t_f] \rightarrow \mathbb{R}^{m_e}$ are the inputs of the pursuer and evader respectively. Let the state constraints at final time t_f be given by

$$\psi(\mathbf{x}(t_f)) = 0 \in \mathbb{R}^p$$

Further, define a generic performance criterion as

$$J(\gamma_p, \gamma_e) = \int_0^{t_f} L(\mathbf{x}(t), \mathbf{u}_p(t), \mathbf{u}_e(t)) dt$$

where $L(\mathbf{x}(t), \mathbf{u}_p(t), \mathbf{u}_e(t))$ is the recurring cost. The pursuer tries to minimize the performance index while the evader tries to maximize it using feedback strategies $\mathbf{u}_p = \gamma_p(\mathbf{x})$ and $\mathbf{u}_e = \gamma_e(\mathbf{x})$. Then the generic versions of Problem 2 and Problem 3 are: find, if such a pair exists, $[\gamma_p^*(\mathbf{x}), \gamma_e^*(\mathbf{x})]$ such that

$$J(\gamma_p^*, \gamma_e^*) = \max_{\gamma_e} \min_{\gamma_p} J(\gamma_p, \gamma_e) = \min_{\gamma_p} \max_{\gamma_e} J(\gamma_p, \gamma_e)$$

For a two player differential game described by the above equations, let $[\gamma_p^*(\mathbf{x}), \gamma_e^*(\mathbf{x})]$ be the feedback saddle-point solutions. Further, let $\mathbf{x}^*(t)$ denote the corresponding state trajectory of the game and $\mathbf{u}_p(t) = \gamma_p(\mathbf{x}(t))$, $\mathbf{u}_e(t) = \gamma_e(\mathbf{x}(t))$ denote the open-loop representations of the feedback strategies.

Theorem 71. *Minimum Principle [1], [14], [5]: There exists a non-zero adjoint vector $\lambda(t) : [0, t_f] \rightarrow \mathbb{R}^n$ satisfying following properties*

$$\begin{aligned}
 \dot{\mathbf{x}}^* &= f(\mathbf{x}^*(t), \mathbf{u}_p^*(t), \mathbf{u}_e^*(t)), \quad \mathbf{x}(0) = \mathbf{x}_0 \\
 \dot{\lambda} &= -\frac{\partial H}{\partial \mathbf{x}}, \quad \lambda(t_f) = \frac{\partial \Phi}{\partial \mathbf{x}} \Big|_{t_f} \\
 (8.1) \quad \frac{\partial H}{\partial \mathbf{u}_p} &= 0, \quad \frac{\partial H}{\partial \mathbf{u}_e} = 0 \quad \text{or} \quad H_0 = \max_{\mathbf{u}_e} \min_{\mathbf{u}_p} H = \min_{\mathbf{u}_p} \max_{\mathbf{u}_e} H
 \end{aligned}$$

where $H = L + \lambda^\top f$ is the system Hamiltonian, $\Phi(t_f, \mathbf{x}(t_f)) = \mu^\top \psi(\mathbf{x}(t_f))$ and $\mu \in \mathbb{R}^p$ are undetermined multipliers at final time.

8.1. Analysis using Hamiltonian. For the system given by (2.1) the Hamiltonian is

$$\begin{aligned}
 (8.2) \quad H &= 1 + \lambda_{p_x} v_p \cos \theta_p + \lambda_{p_y} v_p \sin \theta_p + \lambda_{p_\theta} v_p w_p \\
 &\quad + \lambda_{e_x} v_e \cos \theta_e + \lambda_{e_y} v_e \sin \theta_e + \lambda_{e_\theta} v_e w_e
 \end{aligned}$$

where $[\lambda_{p_x} \ \lambda_{p_y} \ \lambda_{p_\theta}]^\top$ denotes the adjoint vector corresponding to the pursuer. Also, let $[\lambda_{e_x} \ \lambda_{e_y} \ \lambda_{e_\theta}]^\top$ denote the adjoint vector corresponding to the evader. Define, $\lambda_p = \sqrt{\lambda_{p_x}^2 + \lambda_{p_y}^2}$, $\lambda_e = \sqrt{\lambda_{e_x}^2 + \lambda_{e_y}^2}$, $\phi_p = \tan^{-1}(\lambda_{p_y}/\lambda_{p_x})$ and $\phi_e = \tan^{-1}(\lambda_{e_y}/\lambda_{e_x})$. Thus we can write (8.2) as

$$\begin{aligned}
 (8.3) \quad H &= 1 + v_p \lambda_p \cos(\theta_p - \phi_p) + \lambda_{p_\theta} v_p w_p \\
 &\quad + v_e \lambda_e \cos(\theta_e - \phi_e) + \lambda_{e_\theta} v_e w_e
 \end{aligned}$$

By Theorem 5 the capture time $T_c(\gamma_p, \gamma_e) = T_a \leq \infty$. Let $\mu = [\mu_x \ \mu_y]^\top$ be the undetermined constants and $\psi(\mathbf{x}(T_a))$ is defined by (2.2). Thus, from Theorem 71,

$$\Phi(\mathbf{x}(T_a)) = \mu^\top \psi(\mathbf{x}(T_a))$$

The adjoint system for pursuer (evader) is given as

$$\begin{aligned}
 (8.4) \quad \dot{\lambda}_{i_x} &= 0 \quad \dot{\lambda}_{i_y} = 0 \\
 \dot{\lambda}_{i_\theta} &= -v_i [-\lambda_{i_x} \sin \theta_i + \lambda_{i_y} \cos \theta_i] \\
 &= v_i \lambda_i \sin(\theta_i - \phi_i)
 \end{aligned}$$

for $i \in \{p, e\}$.

Lemma 72. *Both the pursuer and evader use input policy $\mathbf{u}_i \in \mathcal{U}_i$ such that $v_i(t) = v_{i_m} \ \forall t \in [0, T_a]$.*

Proof. From Theorem 70, the capture occurs at the boundary of the left reachable set or the right reachable set. From (3.1) it is seen that the boundary of the left and right reachable set is characterized by the input policy $\mathbf{u}_i \in \mathcal{U}_i$ such that $v_i(t) = v_{i_m} \ \forall t$. \square

Lemma 73. *Any optimal path corresponding to the saddle point strategy for the pursuer (evader) is the concatenation of arcs of circles of radius r_p (r_e) and line segments, all parallel to some fixed direction ϕ_p (ϕ_e).*

Proof. The statement is derived using (8.1). The Hamiltonian is affine in $w_p(t)$ and $w_e(t)$. If $\lambda_{p_\theta}(t) = 0$ for all $t \in [t_1, t_2] \subseteq [0, T_a]$ then from (8.4) we must have $\dot{\lambda}_{p_\theta}(t) = 0 = v_p(t) \lambda_p(t) \sin(\theta_p(t) - \phi_p)$. Thus $\theta_p(t) = \phi_p$ or $\theta_p(t) = \phi_p + \pi$ for all $t \in [t_1, t_2] \subseteq [0, T_a]$ and the path is a line segment with direction ϕ_p . Thus $w_p(t) = 0$ for all $t \in [t_1, t_2] \subseteq [0, T_a]$. If $|\lambda_{p_\theta}| > 0$, this would imply that $w_p(t) = \pm w_{p_m}$ and the path would be an arc of circle $A_p(t)$ or $C_p(t)$. Thus H will be minimized with respect to $w_p(t)$ only if $w_p(t) = 0$ or $w_p(t) = \pm w_{p_m}$.

Similar arguments can be used to prove the claim for the evader, where instead of minimizing H we need to maximize H with respect to $w_e(t)$. \square

Proposition 74. *The straight line paths that are followed by both pursuer and evader are parallel to each other i.e. $\phi_p = \phi_e$.*

Proof. By Theorem 71, $\lambda_{p_x}(T_a) = \frac{\partial \Phi}{\partial x_p} = \mu_x$, $\lambda_{p_y}(T_a) = \frac{\partial \Phi}{\partial y_p} = \mu_y$, and $\phi_p(T_a) = \tan^{-1}(\mu_y/\mu_x)$. Similarly we can show, $\lambda_{e_x}(T_a) = \frac{\partial \Phi}{\partial x_e} = -\mu_x$, $\lambda_{e_y}(T_a) = \frac{\partial \Phi}{\partial y_e} = -\mu_y$, $\phi_e(T_a) = \tan^{-1}(\mu_y/\mu_x)$. Further, from (8.4), $\lambda_{p_x}, \lambda_{p_y}, \lambda_{e_x}, \lambda_{e_y}$ are constants. Thus we can conclude that $\phi_p(t) = \phi_e(t) = \tan^{-1}(\mu_y/\mu_x)$ for all time t . \square

Thus from the Hamiltonian formalism we have concluded that the trajectories are either minimum turning radius circles or straight lines parallel to some fixed line.

Theorem 75. *If $d_{pe}^0 \geq 2r_e + 2\pi r_e(v_{p_m}/v_{e_m})$ then the saddle-point strategies of the pursuer and the evader result in pursuer and evader trajectories being coincident to circles in an PE -pairs and one of the common tangents of that pair.*

Proof. By Theorem 70, the strategies of both the pursuer and the evader are of the type CS . Thus the capture takes place along the straight line path. However, from Proposition 74 it was shown that the straight lines are parallel. Thus if the capture must occur along the straight lines, the lines must be coincident. Since, both the pursuer and the evader travel along the circle and straight line the paths must be the common tangents to circles in one of the PE -pair. \square

9. FEEDBACK LAW USING GEOMETRY

In this section we design algorithms to select an appropriate tangent which is the open-loop representation of feedback saddle-point strategies. As discussed in Section 3.1 each PE -pair has four common tangents. Since there are four such PE -pairs we will have 16 directed tangents in total. First we show that at any time t , only one directed tangent corresponding to each PE -pair in the set $PE(t)$ is a valid tangent along which the saddle-point trajectories may occur. Next we give an algorithm to find the time of capture for the valid tangent on each of the PE -pairs. Finally, we formulate a matrix game at each instant of time to design feedback saddle-point strategies for the pursuit-evasion game.

9.1. Selection of valid tangent corresponding to each PE -pair.

Lemma 76. *At each time t , corresponding to each pair of PE -circles in the set $PE(t)$ there is only one valid common tangent with which saddle point strategies can coincide.*

Proof. We prove this on a case by case basis. Consider a circle pair $\{A_p(t), C_e(t)\} \in PE(t)$ as shown in Figure 3.1. A directed straight line $\overrightarrow{O_p O_e}$ is drawn from the center of circle A_p to the center of circle C_e . Clearly, the tangents which end on the evader to the right of $\overrightarrow{O_p O_e}$ are not feasible as the direction of the tangents do not match with the orientation of the evader. Similarly, the tangents which end on $C_e(t)$ to the left of the line $\overrightarrow{O_p O_e}$ are also not feasible. Hence, we can eliminate tangents T_1, T_2 and T_4 . Thus, only the tangent T_3 (dashed line) is a feasible one. Similarly, the claim can be proven for other pairs in the set $PE(t)$. \square

Algorithm 1 is designed to compute the valid tangent for each PE -pair. The common tangents of all the PE -pairs have been shown in Figures 3.1, 9.1, 9.2, and 9.3. In each case the valid tangent has been shown by a dashed line.

Algorithm 1 Valid Tangent

- (1) For the tangent under consideration let T_p be its intersection point with the pursuer circle under consideration and T_e be the intersection point with the evader circle under consideration.
- (2) The following observations can be seen from Figures 3.1, 9.1, 9.2, and 9.3 for valid tangent.
 - (a) For $A_p(t)$ and $A_e(t)$ the angle between the valid tangent and $\overrightarrow{O_p T_p}$ and $\overrightarrow{O_e T_e}$ translated to T_p and T_e respectively is $\pi/2$ in anti-clockwise direction.
 - (b) For $C_p(t)$ and $C_e(t)$ the angle between the valid tangent and $\overrightarrow{O_p T_p}$ and $\overrightarrow{O_e T_e}$ translated to T_p and T_e respectively is $-\pi/2$ in anti-clockwise direction.
- (3) For a given directed tangent \vec{T} in a PE -pair if the angles with $\overrightarrow{O_p T_p}$ and $\overrightarrow{O_e T_e}$ satisfy the conditions above then it is a valid tangent.

Algorithm 2 Algorithm to compute time to capture along a valid tangent for $\{A_p(t), C_e(t)\}$ pair

Input: Valid tangent for the pair $\{A_p(t), C_e(t)\}$

Let ET_e be the arc subtended between $O_e E$ and $O_e T_e$ in clockwise direction and let PT_p be the arc subtended by $O_p P$ and $O_p T_p$ in anticlockwise direction as shown in Figure 3.1. Compute the length of the arcs $PT_p = l_{ap}$ and $ET_e = l_{ae}$ and define $t_p := l_{ap}/v_{p_m}$ and $t_e := l_{ae}/v_{e_m}$. Also, let the distance between $T_p T_e$ be denoted by d .

- (1) If $t_p > t_e$ the evader will come out of the circle and onto the tangent earlier than the evader.
 - (a) $\tilde{t} := t_p - t_e$. Thus the evader will travel a distance $d_e := v_{e_m} \tilde{t}$ on the straight line before the pursuer comes onto the tangent.
 - (b) Thus at the time t_p the distance between the pursuer and evader will be $\tilde{d} := d + d_e$. Now the time to capture from this point will be $\bar{t} := \tilde{d}/(v_{p_m} - v_{e_m})$.
 - (c) Thus the time to capture will be $T_{ac}(t) = t_p + \bar{t}$.
- (2) If $t_p \leq t_e$ the pursuer will come on straight line earlier.
 - (a) $\tilde{t} := t_e - t_p$. Thus the pursuer will travel a distance $d_p := v_{p_m} \tilde{t}$ on the straight line before the evader comes on the straight line.
 - (b) Thus at the time t_e the distance between the pursuer and evader will be $\tilde{d} := d - d_p$. Now the time to capture from this point will be $\bar{t} := \tilde{d}/(v_{p_m} - v_{e_m})$.
 - (c) Thus the time to capture will be $T_{ac}(t) = t_e + \bar{t}$.

Output: Time to capture along a valid tangent for $\{A_p(t), C_e(t)\}$ pair = $T_{ac}(t)$

9.2. Algorithm for selecting the correct PE -pair. It was shown, using geometry, in Lemma 76 that each PE -pair has only one valid tangent. Thus there are four valid tangents (one corresponding to each PE -pair) with which the saddle-point strategies of the pursuit-evasion game may coincide.

Recall that the clockwise circle $C_p(t)$ is traversed for $w_p(t) = -w_{p_m}$ and anticlockwise circle $A_p(t)$ for $w_p(t) = +w_{p_m}$. Similarly, for the evader the clockwise circle $C_e(t)$ is traversed for $w_e(t) = -w_{e_m}$ and anticlockwise circle $A_e(t)$ for $w_e(t) = +w_{e_m}$. Selecting $w_p(t) = +w_{p_m}$ and $w_e(t) = -w_{e_m}$ is equivalent to selecting the valid tangent of the pair $\{A_p(t), C_e(t)\}$ along which saddle-point strategies for the pursuit-evasion game will occur. The computation of time to capture at time t , $T_{ac}(t)$, for the valid tangent of the pair $\{A_p(t), C_e(t)\}$, shown in Figure 3.1, is given in Algorithm 2.

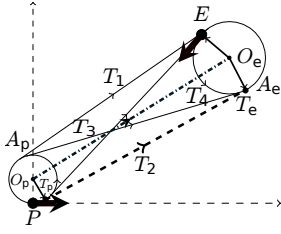


FIGURE 9.1. $\{A_p(t), A_e(t)\}$

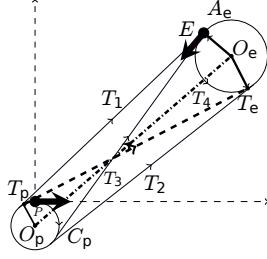


FIGURE 9.2. $\{C_p(t), A_e(t)\}$

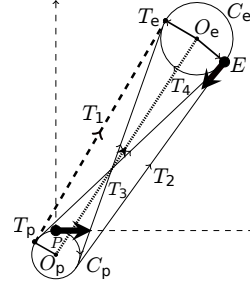


FIGURE 9.3. $\{C_p(t), C_e(t)\}$

$P \setminus E$	$w_e(t) = +w_{e_m}$	$w_e(t) = -w_{e_m}$
$w_p(t) = +w_{p_m}$	$T_{aa}(t)$	$T_{ac}(t)$
$w_p(t) = -w_{p_m}$	$T_{ca}(t)$	$T_{cc}(t)$

TABLE 1. Matrix game at time instant t

Similarly, we calculate the times corresponding to each circle pairs and hence each input pairs. At an given time instant, say t , let $A_p(t)$, $C_p(t)$, and $A_e(t)$, $C_e(t)$ be the pursuer and evader circles respectively. Let $T_{aa}(t)$, $T_{ac}(t)$, $T_{ca}(t)$ and $T_{cc}(t)$ be the times corresponding to valid tangents of circle-pairs $\{A_p(t), A_e(t)\}$, $\{A_p(t), C_e(t)\}$, $\{C_p(t), A_e(t)\}$, and $\{C_p(t), C_e(t)\}$ respectively. For example, if the pursuit-evasion saddle-point occurs on the PE -pair $\{A_p(t), C_e(t)\}$ then at t we must have $w_p(t) = w_{p_m}$ and $w_e(t) = -w_{e_m}$ initially. Similarly we have,

- (1) $\{A_p(t), A_e(t)\} \Rightarrow w_p(t) = +w_{p_m}, w_e(t) = +w_{e_m}$
- (2) $\{A_p(t), C_e(t)\} \Rightarrow w_p(t) = +w_{p_m}, w_e(t) = -w_{e_m}$
- (3) $\{C_p(t), A_e(t)\} \Rightarrow w_p(t) = -w_{p_m}, w_e(t) = +w_{e_m}$
- (4) $\{C_p(t), C_e(t)\} \Rightarrow w_p(t) = -w_{p_m}, w_e(t) = -w_{e_m}$

until the time that the trajectory leaves the corresponding circle and starts on the straight line path along the common tangent. Thus corresponding to pursuer and evader inputs at time t , we obtain times of capture along each of the valid tangents. Using these times we formulate a matrix game as shown in Table 1. The valid tangent on which the pursuit-evasion game occurs constitutes the open-loop saddle point strategies for the pursuit-evasion differential game. Thus, starting at time t with the configuration $\mathbf{p}(t)$, $\mathbf{e}(t)$, the saddle-point solution of the matrix game at each instant t will give the common tangent, with which the open-loop representation of the feedback saddle-point strategies is coincident. Thus the policy of the evader would be max – min solution of the matrix game while that of the pursuer would be min – max solution of the matrix game at each instant t . From this discussion we propose the following theorem.

Theorem 77. *If $d_{pe}^0 \geq 2r_e + 2\pi r_e(v_{p_m}/v_{e_m})$, the tangents selected by the saddle-point equilibrium in the matrix game described by Table 1 will be coincident with the open-loop representation of feedback saddle-point strategies at each time $t \geq 0$.*

Saddle point feedback strategies are of prime importance to make the solution robust to non-optimal pursuer/evader policies and external disturbances. If the open-loop solution is computed at each instant of time t and the input value corresponding to time instant t i.e. $w_p(t)$ and $w_e(t)$ is applied then it constitutes

a feedback law. Using Theorem 77, such a feedback law $F(\mathbf{x}(t)) : \mathbf{x}(t) \in \mathbb{R}^6 \rightarrow [\mathbf{u}_p^\top(t) \ \mathbf{u}_e^\top(t)]^\top \in \mathbb{R}^4$ can be described as Algorithm 3.

Algorithm 3 Feedback $[\mathbf{u}_p^\top(t) \ \mathbf{u}_e^\top(t)]^\top = F(\mathbf{x}(t))$

Input: Pursuer state $\mathbf{p}(t)$ and Evader state $\mathbf{e}(t)$

- (1) Given the pursuer and evader states $\mathbf{p}(t)$ and $\mathbf{e}(t)$ at time t compute the circles $C_p(t), C_e(t), A_p(t), A_e(t)$.
- (2) Calculate the tangents corresponding to each pair of circles in $PE(t)$.
- (3) Use Algorithm 1 to obtain the four valid tangents out of 16 common tangents.
- (4) Use Algorithm 2 to compute time to capture for each of the valid tangents and formulate the matrix game at time t as shown above.
- (5) Find $w_p(t)$ as the min – max solution of the matrix game and $w_e(t)$ as the max – min solution of the matrix game.
- (6) At each instant t use $v_p(t) = v_{p_m}$ and $v_e(t) = v_{e_m}$.

Output: $\mathbf{u}_p(t) = [w_p(t) \ v_{p_m}]^\top$ and $\mathbf{u}_e(t) = [w_e(t) \ v_{e_m}]^\top$

10. COMPARISON WITH NUMERICAL SIMULATIONS

In [10], the authors have proposed an algorithm to solve pursuit-evasion games numerically. This is achieved by first solving the min problem of the pursuer and then the max problem of the evader. This optimal problems are solved iteratively to obtain the min – max solution of the differential game. We use their algorithm to numerically solve the game of two cars and the min and the max problems are solved using direct numerical optimal control methods [3] using IPOPT [27]. Clearly, such numerical techniques are not practical for computing feedback solution in real time due to time complexity and convergence issues of numerical optimization methods. However, we do these simulations in order to verify the correctness of the matrix law.

The parameters for the pursuer and evader used for simulations are $v_{p_m} = 2, w_{p_m} = 2, v_{e_m} = 1$ and $w_{e_m} = 1$. The simulations were performed using numerical techniques (NT) as well as the matrix law (ML) for following initial states of the pursuer and the evader:

- (1) $\mathbf{p}_0 = [0, 0, \pi/2], \mathbf{e}_0 = [-3, -6, \pi/2]$ (ML: Figure 10.1, NT: Figure 10.5)
- (2) $\mathbf{p}_0 = [0, 0, \pi/2], \mathbf{e}_0 = [6, 3, \pi/2]$ (ML: Figure 10.2, NT: Figure 10.6)
- (3) $\mathbf{p}_0 = [0, 0, \pi/2], \mathbf{e}_0 = [0, -6, \pi/2]$ (ML: Figure 10.3, NT: Figure 10.7)
- (4) $\mathbf{p}_0 = [0, 0, \pi/2], \mathbf{e}_0 = [0, 6, \pi/2 + \pi/6]$ (ML: Figure 10.4, NT: Figure 10.8)

In all the figures the pursuer trajectory is shown by the dashed curve whereas the evader trajectory is shown by the dotted curve. The comparison of matrix law and the numerical simulation show that the trajectories are identical.

11. CONCLUSION

In this work we have derived a characterization of time optimal pursuit evasion game between two Dubins vehicles using continuous subsets of reachable sets. Using this sets we show that the time optimal saddle point strategies of both the pursuer and evader are circle and a straight line. Using this characterization, we have derived feedback saddle point strategies for the game of two cars. The solutions are computed

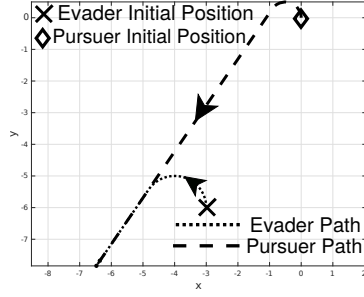


FIGURE 10.1. Feedback law-1

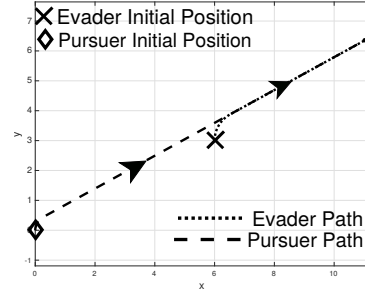


FIGURE 10.2. Feedback law-2

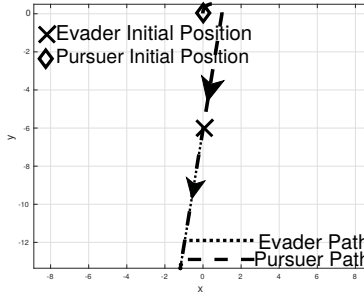


FIGURE 10.3. Feedback law-3

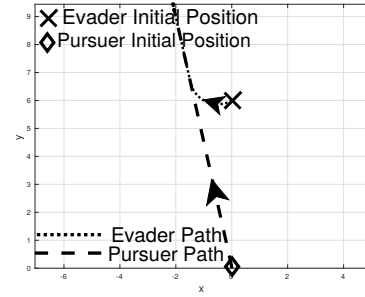


FIGURE 10.4. Feedback law-4

geometrically with insignificant computational effort. Though we have presented $F(\mathbf{x}(t))$ as a continuous time state feedback, any implementation of our algorithm will involve discretization of time and evaluation of Algorithm 3 ($F(\mathbf{x}(t))$) at discrete intervals. Due to the simplicity of the computation, the evaluation of $F(\mathbf{x}(t))$ can be completed for small discretization intervals. A quantitative study on the effect of discretization on the path optimality, however, remains a topic of further research. Simulations using the proposed law show agreement with the solution obtained by solving the pursuit evasion game numerically. Future work includes deriving feedback laws for the case when the evader is very close to the pursuer and for other configurations where capture is possible.

12. APPENDIX

In this section we give proof of Lemma 17. In order to do this we define a kinematic point. A kinematic point can turn instantaneously and move with velocity v_m . The equations governing the motion of the kinematic point are:

$$\begin{aligned} \dot{x}(t) &= v_m \cos(\theta(t)) \\ \dot{y}(t) &= v_m \sin(\theta(t)) \end{aligned}$$

The movement of the kinematic point is also referred to as simple motion in literature (see [14] for details). The reachable set of such a kinematic point, denoted by $R^k(\mathbf{p}_0, \bar{t})$ at time \bar{t} , is a circle of radius $v_m \bar{t}$ located at \mathbf{p}_0 . We consider two kinematic points:

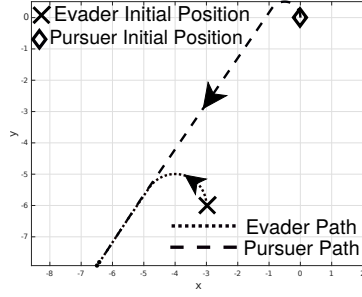


FIGURE 10.5. [19]Numerical -1

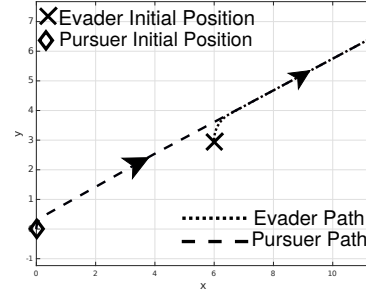


FIGURE 10.6. [19]Numerical -2

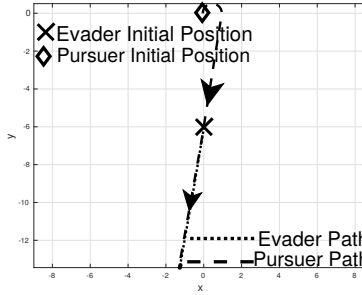


FIGURE 10.7. [19]Numerical -3

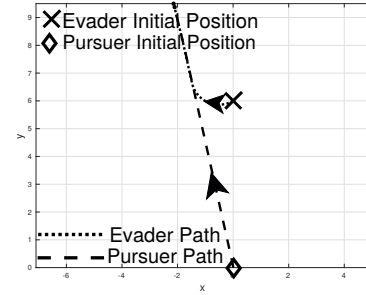


FIGURE 10.8. [19]Numerical -4

- (1) A kinematic point located at the same position as the pursuer (Dubins vehicle) and having maximum velocity v_{p_m} . We refer to this kinematic point as the kinematic pursuer. This kinematic pursuer stays at point \mathbf{p}_0 for $t \in [0, \tilde{t}]$. It starts moving at $t = \tilde{t}$. Thus at time $t > \tilde{t}$ its reachable set $R_p^k(\mathbf{p}_0, t)$ will be a circle of radius $v_{p_m}(t - \tilde{t})$ with center at \mathbf{p}_0 .
- (2) A second kinematic point located at the same position as the evader (Dubins vehicle) and having maximum velocity v_{e_m} . We refer to this kinematic point as the kinematic evader. The kinematic evader starts moving at $t = 0$. Thus its reachable set at time t , $R_e^k(\mathbf{e}_0, t)$, will be a circle of radius $v_{e_m}t$.

The following result is known [7]:

Lemma 78. *The reachable set of any Dubins vehicle moving with maximum velocity v_m is contained inside the reachable set of kinematic point moving with velocity v_m .*

Lemma 79. *For any initial pursuer position $\mathbf{p}_0 \in \mathbb{R}^3$ and any initial evader position $\mathbf{e}_0 \in \mathbb{R}^3$ and for all $\tilde{t} < \infty$ there exists $\bar{t} < \infty$ such that the reachable set of the kinematic evader $R_e^k(\mathbf{e}_0, \bar{t})$ is contained inside the reachable set of the kinematic pursuer $R_p^k(\mathbf{p}_0, \bar{t})$ starting with a delay of \tilde{t} .*

Proof. Let the initial distance between the kinematic pursuer and the kinematic evader be d_{pe}^0 . At time \tilde{t} , point A is the farthest point from the pursuer in evader's reachable set and is located on a straight line joining the evader and the pursuer as shown in Figure 12.1. Thus, for the lemma to hold there must exist a time t s.t. the reachable set of the pursuer has radius greater than $d_{pe}^0 + v_{e_m}t$ i.e. $v_{p_m}(t - \tilde{t}) \geq d_{pe}^0 + v_{e_m}t$. This implies that $(v_{p_m} - v_{e_m})t \geq d_{pe}^0 + v_{p_m}\tilde{t}$. Now the right hand side of the equation is always a finite quantity and since $v_{p_m} > v_{e_m}$ there exists a time $t = \bar{t}$ such that the inequality holds. \square

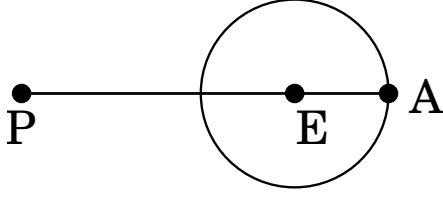


FIGURE 12.1. Farthest point at time \tilde{t}

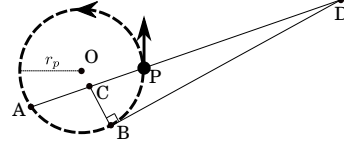


FIGURE 12.2. Point reached by left reachable set after some delay

Lemma 80. Let $\tilde{R}_p^k(\mathbf{p}_0, t) := R_p^k(\mathbf{p}_0, t)/A_p(0)$ i.e. the set of points contained in the reachable set of kinematic pursuer except those which belong to the anti-clockwise pursuer circle. For any initial pursuer position $\mathbf{p}_0 \in \mathbb{R}^3$ and any initial evader position $\mathbf{e}_0 \in \mathbb{R}^3$ the set $\tilde{R}_p^k(\mathbf{p}_0, t)$ of the kinematic pursuer, starting to move at time $\tilde{t} = (2\pi + 2)r_p/v_{p_m}$, is contained inside the left reachable set of the pursuer having the kinematics of a Dubins vehicle and starting at $t = 0$ for all $t \geq \tilde{t}$.

Proof. Let the pursuer (Dubins vehicle) be located at point P with orientation as shown in Figure 12.2. The dotted circle shown in Figure 12.2 is the left minimum turning radius circle of the pursuer. Also, let D be a point located outside the left pursuer circle as shown in Figure 12.2. The kinematic point is also located at P and stays at point P up to time $\tilde{t} = (2\pi + 2)r_p/v_{p_m}$. Thus, the minimum time required for this kinematic pursuer to reach point D, say t_1 , is time it stays at point P ($t \in [0, \tilde{t}]$) plus time required to cover distance PD. Thus, $t_1 = \tilde{t} + \hat{t}_1$, where $\hat{t}_1 = \text{len}(PD)/v_{p_m}$ (since it is constrained to stay at P for time $t \in [0, \tilde{t}]$).

Now the minimum time required by CS type of curve given by (3.1) to reach point D is given by

$$t_2 = \{\text{len}(\text{Arc } PAB) + \text{len}(BD)\}/v_{p_m}$$

Since $\text{len}(\text{Arc } PAB) \leq 2\pi r_p$, $\text{len}(BD) \leq \text{len}(AD)$, and $\text{len}(AD) \leq 2r_p + \text{len}(PD)$,

$$\begin{aligned} t_2 &\leq (2\pi r_p + \text{len}(AD))/v_{p_m} \\ &\leq (2\pi r_p + 2r_p + \text{len}(PD))/v_{p_m} \\ &= \hat{t}_1 + (2\pi + 2)r_p/v_{p_m} = t_1 \end{aligned}$$

Thus $t_2 \leq t_1$ and the claim follows. □

Lemma 81. If $d_{pe}^0 \geq 2r_p + 2\pi r_p(v_{e_m}/v_{p_m})$ the pursuer can intercept the evader before it enters anti-clockwise pursuer circle by the trajectories of the type LS.

Proof. Let the pursuer be located at a distance d_{pe}^0 away from the evader. By the arguments similar to those used in Lemma 45 we can conclude that the evader requires at least time $t_e := [d_{pe}^0 - 2r_p]/v_{e_m}$ to reach any point on the pursuer's circle.

Any point on the left pursuer circle can be reached by the pursuer in time $t \leq t_p := 2\pi r_p/v_{p_m}$. Hence if t_p is less than the minimum time in which the evader can reach any point on the pursuer circles then the pursuer can intercept the evader before it can enter the anti-clockwise pursuer circle. Thus, if

$$\begin{aligned} t_e &\geq t_p \\ [d_{pe}^0 - 2r_p]/v_{e_m} &\geq 2\pi r_p/v_{p_m} \\ d_{pe}^0 &\geq 2r_p + 2\pi r_p(v_{e_m}/v_{p_m}) \end{aligned}$$

the claim follows. \square

Proof of Lemma 17. By Lemma 81, even if the evader's reachable set can extend into the anti-clockwise pursuer circle this part of evader's reachable set cannot form a part of $R_e^-(\mathbf{e}_0, R_p^l, T_l)$ if $d_{pe}^0 \geq 2r_p + 2\pi r_p(v_{e_m}/v_{p_m})$. Similarly, from Lemma 80 we have that the set $\bar{R}_p^k(\mathbf{p}_0, t)$ of kinematic pursuer is contained inside the reachable set of pursuer. Further, at time \bar{t} the kinematic pursuer's reachable set contains the reachable set of the kinematic evader (by Lemma 79) and hence the reachable set of the evader (by Lemma 78). This implies that the reachable set of the evader is contained inside the left reachable set of the pursuer.

REFERENCES

1. Tamer Başar and Geert Jan Olsder, *Dynamic noncooperative game theory*, SIAM, 1998.
2. Ritwik Bera, Venkata Ramana Makkapati, and Mangal Kothari, *A comprehensive differential game theoretic solution to a game of two cars*, Journal of Optimization Theory and Applications **174** (2017), no. 3, 818–836.
3. J. Betts, *Practical methods for optimal control and estimation using nonlinear programming*, second ed., Society for Industrial and Applied Mathematics, 2010.
4. Jean-Daniel Boissonnat, André Cérézo, and Juliette Leblond, *Shortest paths of bounded curvature in the plane*, Journal of Intelligent and Robotic Systems **11** (1994), no. 1-2, 5–20.
5. Arthur Earl Bryson, *Applied optimal control: optimization, estimation and control*, CRC Press, 1975.
6. Xuân-Nam Bui and Jean-Daniel Boissonnat, *Accessibility region for a car that only moves forwards along optimal paths*, Ph.D. thesis, INRIA, 1994.
7. EJ Cockayne and GWC Hall, *Plane motion of a particle subject to curvature constraints*, SIAM Journal on Control **13** (1975), no. 1, 197–220.
8. Ernest Cockayne, *Plane pursuit with curvature constraints*, SIAM Journal on Applied Mathematics **15** (1967), no. 6, 1511–1516.
9. Lester E Dubins, *On curves of minimal length with a constraint on average curvature, and with prescribed initial and terminal positions and tangents*, American Journal of mathematics **79** (1957), no. 3, 497–516.
10. H. Ehtamo and T. Raivio, *On applied nonlinear and bilevel programming or pursuit-evasion games*, Journal of Optimization Theory and Applications **108** (2001), no. 1, 65–96.
11. I. Exarchos and P. Tsiotras, *An asymmetric version of the two car pursuit-evasion game*, 53rd IEEE Conference on Decision and Control, 2014.
12. Ioannis Exarchos, Panagiotis Tsiotras, and Meir Pachter, *On the suicidal pedestrian differential game*, Dynamic Games and Applications **5** (2015), no. 3, 297–317.
13. Haomiao Huang, Wei Zhang, Jerry Ding, Dušan M Stipanović, and Claire J Tomlin, *Guaranteed decentralized pursuit-evasion in the plane with multiple pursuers*, 50th IEEE Conference on Decision and Control and European Control Conference, 2011.
14. R. Isaacs, *Differential games*, Dover Publications, 1999.
15. Jung Soon Jang and Claire J Tomlin, *Control strategies in multi-player pursuit and evasion game*, AIAA Guidance, Navigation, and Control Conference and Exhibit **6239** (2005), 15–18.
16. A. W. Merz, *The game of two identical cars*, Journal of Optimization Theory and Applications **9** (1972), no. 5, 324–343.
17. Koichi Mizukami and Kenichi Eguchi, *A geometrical approach to problems of pursuit-evasion games*, Journal of the Franklin Institute **303** (1977), no. 4, 371–384.
18. Selina Pan, Haomiao Huang, Jerry Ding, Wei Zhang, Claire J Tomlin, et al., *Pursuit, evasion and defense in the plane*, American Control Conference, 2012.
19. Tuomas Raivio and Harri Ehtamo, *On the numerical solution of a class of pursuit-evasion games*, pp. 177–192, Birkhäuser Boston, 2000.
20. U. Ruiz, R. Murrieta-Cid, and J. L. Marroquin, *Time-optimal motion strategies for capturing an omnidirectional evader using a differential drive robot*, IEEE Transactions on Robotics **29** (2013), no. 5, 1180–1196.
21. Ubaldo Ruiz and Rafael Murrieta-Cid, *A differential pursuit/evasion game of capture between an omnidirectional agent and a differential drive robot, and their winning roles*, International Journal of Control **89** (2016), no. 11, 2169–2184.
22. P. Soueres, A. Balluchi, and A. Bicchi, *Optimal feedback control for route tracking with a bounded-curvature vehicle*, International Journal of Control **74** (2001), no. 10, 1009–1019.

23. Philippe Soueres and J-P Laumond, *Shortest paths synthesis for a car-like robot*, IEEE Transactions on Automatic Control **41** (1996), no. 5, 672–688.
24. W. Sun, P. Tsiotras, T. Lolla, D. N. Subramani, and P. F. J. Lermusiaux, *Pursuit-evasion games in dynamic flow fields via reachability set analysis*, American Control Conference, 2017.
25. Wei Sun and Panagiotis Tsiotras, *Pursuit evasion game of two players under an external flow field*, American Control Conference, 2015.
26. Héctor J Sussmann and Guoqing Tang, *Shortest paths for the reeds-shepp car: a worked out example of the use of geometric techniques in nonlinear optimal control*, Rutgers Center for Systems and Control Technical Report **10** (1991), 1–71.
27. Andreas Wachter and Lorenz T. Biegler, *On the implementation of an interior-point filter line-search algorithm for large-scale nonlinear programming*, Mathematical Programming **106** (2006), no. 1, 25–57.